THESIS

SWEET SURPRISE: THE SEARCH FOR GENES CONFERRING BEET CURLY TOP VIRUS RESISTANCE

Submitted by

Jordan Withycombe

Department of Agricultural Biology

In partial fulfillment of the requirements

For the Degree of Master of Science

Colorado State University

Fort Collins, Colorado

Fall 2023

Master's Committee:

Advisor: Punya Nachappa

Vamsi Nalam
Marc Nishimura
Kevin Dorn

ABSTRACT

SWEET SURPRISE: THE SEARCH FOR GENES CONFERRING BEET CURLY TOP VIRUS RESISTANCE

Sugar beets (*Beta vulgaris* L.) are grown across the western United States and suffer economic loss annually to curly top disease. Curly top disease is caused by the beet curly top virus (BCTV) and is spread by the only known insect vector the beet leafhopper, Circulifer tenellus Baker (BLH). Current management strategies for BCTV include chemical control using neonicotinoid seed treatments and foliar insecticidal sprays, as well as the use of BCTV-resistant sugar beet varieties. However, the underlying genetic mechanism surrounding resistance in sugar beet is unknown. The overarching goal of this study was to identify the mechanism of resistance in sugar beet to BCTV and identify potential genes conferring resistance. The objectives for this study were: 1) classify the nature of BCTV resistance in a resistant (EL10) and susceptible (FC709-2) genotype of sugar beet using host suitability and host preference insect assays, as well as assess viral load within each genotype and 2) characterize the transcriptional response to BCTV infection using RNA-sequencing.

To classify the nature of BCTV resistance in each genotype of sugar beet, host suitability and preference assays were conducted using virus infected and uninfected BLH. In host suitability assays, the percentage of surviving BLH adults and the number of nymphs produced when reared on a single plant of either genotype was determined over a 3-week period. There was no difference in adult survival, or the number of nymphs produced on either genotype for the virus infected or uninfected leafhoppers. Host preference assays were used to assess settling

behavior of BLH over time when given a choice between the two genotypes. It was concluded that virus infected leafhoppers had a clear choice to settle on the susceptible genotype at all timepoints after 4 hours, while uninfected leafhoppers did not make as strong of a settling choice. Average viral load for each genotype across three timepoints was estimated using qPCR. The results showed that the average viral load increased in each genotype over time, yet there was no difference in the average viral load between the genotypes at any individual timepoint.

The global transcriptional response to BCTV infection over time for a resistant and susceptible genotype of sugar beet was conducted using RNA-sequencing technology. Mock-inoculated and BCTV-inoculated plants from each genotype were sampled on day 1, 7 or 14 post inoculation resulting in the preparation of 36 mRNA sequencing libraries. Comparison between mock-inoculated and BCTV-inoculated plants of each genotype and timepoint were conducted separately to generate six list of differentially expressed transcripts (DETs). Each transcript was annotated with a description and further classified for its role in the plant biological, cellular or molecular processes. The results showed that both genotypes of sugar beet had a dynamic response to BCTV infection over time, although there was minimal overlap between the responses to one another. EL10, the resistant genotype, had DETs associated with phytohormone production including jasmonic acid and abscisic acid, along with proteins linked to stress reduction and the downregulation of plant primary metabolic processes. In contrast FC709-2, the susceptible genotype, was found to produce opposing phytohormones like salicylic acid and auxins, as well as the production of volatile organic compounds and an increase of primary plant metabolic processes. These opposing responses shed light on the differences in the transcriptional response of a resistant and susceptible genotype of sugar beet. Understanding and classifying the mechanisms of resistance or susceptibility to BCTV infection in sugar beet is

beneficial to researchers and plant breeders as it provides a basis for further exploration of the host plant-virus-vector interactions.

ACKNOWLEDGEMENTS

First and foremost, I am extremely thankful for my advisor, Dr. Punya Nachappa, for the guidance and support she showed me throughout this journey. I will forever cherish the mentorship and wisdom she gave me throughout this time. She exemplifies true dedication to research within the field of virus-vector-host plant interactions and will continue to inspire me.

I am also particularly appreciative of the contributions of my committee members, Dr. Vamsi Nalam, Dr. Marc Nishimura, and Dr. Kevin Dorn. They provided insightful feedback and different perspectives that helped to elevate the quality of my research and writing.

All the lab members of the Nachappa lab, both past and present, have contributed to my success as a researcher and I am fortunate to have worked and most importantly learned from them all. I owe a special thanks to Laine Hackenburg for being an incredible friend and fellow concert attendee during this time.

My family and friends back home deserve a special mention for their steady encouragement and support while I ventured out of my comfort zone to complete this degree. The conversations over the years between us brought me peace and motivation throughout this adventure.

Finally, I would like to thank my loving partner, Erik, for his endless support. May he forever know the special role he played while I chased this dream.

TABLE OF CONTENTS

ABSTRACT ii
ACKNOWLEDGEMENTS v
LIST OF TABLES viii
LIST OF FIGURES ix
INTRODUCTION 1
Sugar beet 1
Curly top disease 2
Symptoms 3
Beet leafhopper 3
BCTV epidemiology 5
Disease management 6
Mechanisms of plant defense to viral pathogens 7
Mechanisms of plant resistance to insects 10
Identification of virus resistance in sugar beet 11
Goals and objectives 12
MATERIALS AND METHODS 13
Sugar beet planting and growing conditions 13
Beet leafhopper colony maintenance 13
DNA extraction and end-point PCR analysis 14
Beet leafhopper host suitability assay 15
Beet leafhopper host preference assay 15
Quantifying viral coat protein copy number in two sugar beet genotypes over time: 16
Virus inoculation and leaf tissue collection 16
Quantitative PCR 16
RNA Sequencing: 17
Plant growth, treatment, and sample collection 17
DNA and RNA extraction and virus presence-absence testing 18
DNase treatment, qubit quantification, and RNA pooling 18
Library preparation 19
Bioinformatic analysis of mRNA reads: 19

Trimming reads 19
Mapping to reference genome 20
Differential expression analysis 20
Functional analysis and gene ontology 20
Weighted Gene Co-expression Network Analysis 21
RESULTS 22
No difference in adult beet leafhopper survival or the number of nymphs produced on either sugar beet genotype 22
Virus-infected leafhoppers prefer to settle on the susceptible genotype rather than the resistant 23
Quantification of BCTV viral load show no difference between genotypes 23
RNA sequencing to investigate transcriptional responses to BCTV in EL10 and FC709-2 24
Quality control of raw reads 24
Differentially expressed transcripts identified for each genotype at three time points 25
Gene ontology terms assigned to each sugar beet genotype in response to virus infection 26
Scanning of DETs for associated protein families 28
Functional grouping of DETS to analyze plant response to virus infection 29
Hormone Signaling 29
Protein production and protein ubiquitination 30
Plant growth and cell cycling 31
Stress reduction of ROS 31
Volatile production in response to insect feeding and virus infection 32
WGCNA 32
DISCUSSION 34
CONCLUSIONS AND FUTURE DIRECTIONS 41
FIGURES AND TABLES 44
REFERENCES 70
APPENDICES 77

LIST OF TABLES

Table 1: Summary statistics of RNA sequencing reads……52
Table 2: EL10 day 1 list of 30 top DETs ……55
Table 3: EL10 day 7 list of 30 top DETs ……56
Table 4: EL10 day 14 list of 30 top DETs ……57
Table 5: FC709-2 day 1 list of 30 top DETs ……58
Table 6: FC709-2 day 7 list of 30 top DETs ……59
Table 7: FC709-2 day 14 list of 30 top DETs ……60

LIST OF FIGURES

Figure 1: BCTV symptoms on sugar beet……...……44
Figure 2: Beet leafhopper…….……..……45
Figure 3: Beet leafhopper migration patterns…...…….……46
Figure 4: RNA sequencing experimental workflow...……..…..…..……47
Figure 5: Host suitability assay……..…...……..……48
Figure 6: Host preference assay…… …...……..……49
Figure 7: Quantification of viral load……...…….……..……50
Figure 8: Range of BCTV symptoms on the two genotypes……..……...…….……51
Figure 9: PCA plot of RNA-seq samples …..…...……...……53
Figure 10: Volcano plots of DETs……..…...…….……54
Figure 11: Upset plot of DETs……...…….……61
Figure 12: GO terms associated with EL10……...…….……62
Figure 13: GO terms associated with FC709-2.....…….……63
Figure 14: Protein family domains identified at day 1 for each genotype ……..……64
Figure 15: Protein family domains identified at day 7 for each genotype ……..……65
Figure 16: Protein family domains identified at day 14 for each genotype ……66
Figure 17: Module-trait relationship heatmap for EL10…….……67
Figure 18: Module-trait relationship heatmap for FC709-2……..……..……68
Figure 19: Summary of the transcriptional response found for each genotype……..……69

INTRODUCTION

Sugar beet

Sugar beet, *Beta vulgaris* L, is an economically important crop grown and processed in the mid-west and western regions of the United States (U.S.). In 2021, the estimated production value of sugar beets was 1.9 billion dollars (USDA Crop Values Summary 2023). Sugar beets are refined into granulated sugar while the biproducts are used as a supplemental livestock feed (Bhattacharya and Lubbadah 1971). According to USDA estimates, beet sugar makes up 55-60% of total U.S. sugar production and around 20% of global sugar production (USDA Crop Values Summary 2023; Hoffmann et al. 2021).

The history of sugar beets in Colorado dates back to the early 1880s (Weeks 2017). Sugar beets quickly grew to be one of the most important agricultural crops in the state by the early 1900s. Many processing factories were built along the front range and western slopes of Colorado, leading to job opportunities and an influx of people to the region. However, the industry was heavily impacted by curly top disease in the 1920s and 30s, which destroyed most of the crop (Bennett 1971; Panella et al. 2014). Sugar beet cultivation was revived through the use of resistant varieties and breeding efforts of the USDA. In the following years, the industry was plagued with a number of other diseases, damaging insects, and high weed pressure that led to a severe reduction in the industry and closure of numerous processing plants (Coons et al. 1955). More recently, sugar beets were genetically modified to exhibit resistance to the herbicide glyphosate and designated as a “Roundup-ready” crop. This modification was quickly adopted by the industry (McGinnis et al. 2010). Current breeding efforts are focused on growers needs

which primarily include increased disease resistance, higher yield and sugar content, and climate adaptive traits.

Curly top disease

Curly top disease is caused by the beet curly top virus (BCTV) and has significant economic impact in agricultural production in the western United States (Bennett 1971; Harveson 2015; Stenger and McMahon 1997; Strausbaugh et al. 2008). The virus can infect approximately 300 different plant species, including several economically important crops such as tomato, bean, spinach, cucurbits, pepper, hemp, and sugar beet (Bennett 1971; Chen and Gilbertson 2016). BCTV belongs to the family *Geminiviridae,* and the genus *Curtovirus* (Chen and Gilbertson 2016).

BCTV is characterized by a monopartite, single-stranded circular DNA genome that is encapsulated within twinned quasi-isometric virion units (Harrison 1985). The BCTV genome is approximately 2.9 kilobases with an intergenic region (IR), three sense open reading frames (ORFs) (V1, V2, and V3) and four complementary sense ORFs (C1, C2, C3 and C4). The three virion-sense ORFs encodes for the coat protein, the DNA regulator, and the movement protein, all of which are highly conserved between strains (Stanley et al. 1986; Soto et al. 2005). The complementary sense ORFs are less conserved and encode for the replication initiator protein (Rep), a replication-enhancer protein (REn), as well as viral proteins associated with the cell cycle, suppression of host defenses and symptom development (Stanley et al. 1986; Latham et al. 1997). Replication of the virus occurs in the nucleus via rolling circle replication using the host plant machinery. After replication, BCTV moves throughout the plant as virion particles and is limited to the phloem (Esau and Hoefert 1973). Systemic infection and plant-to-plant movement

are highly correlated with functional coat proteins, as this is required for virus uptake and transmission by the insect vector (Stanley et al. 1986; Soto et al. 2005).

There are 11 recognized strains of BCTV including: California/Logan (CA/Logan), Colorado (CO), Kimberly1 (Kim1), Leafhopper 71 (LH71), Mild (Mld), Pepper curly top (PeCT), Pepper yellow dwarf (PeYD), Severe (Svr), Severe pepper (SvrPep), Spinach curly top (SpCT), and Worland (Wor) (Strausbaugh et al. 2017). The prevalence of each strain varies over time by geographical region and typically are observed as co-infection within a single plant (Strausbaugh et al. 2017).

Symptoms

BCTV induces a wide range of symptoms in sugar beet including stunted growth and chlorosis of the whole plant, and the crinkling, cupping, and upward curling of leaves (Figure 1) (Ball 1917; Bennett 1971; Esau 1976; Chen and Gilbertson 2016). On the underside of the leaf, veins may become enlarged and ridged, along with small tumorous growths (Ball 1917; Esau 1976; Bennett 1971). There is often necrosis of phloem tissue that can be observed in the taproot as dark concentric rings (Ball 1917). Symptomology can differ dramatically depending on the infecting strain and host plant and may range from mild to severe (Strausbaugh et al. 2017).

Beet leafhopper

The beet leafhopper (BLH), *Circulifer tenellus* Baker, is the only known insect vector of BCTV (Figure 2) (Ball 1917; Bennett 1971). This species of leafhopper is in the family Cicadellidae under the order Hemiptera. This order is characterized by having elongated piercing sucking mouthparts for penetrating plant cells and ingesting the contents (Schuh and Slater 1995). Beet leafhoppers are primarily found in semiarid climates, specifically in the western and southwestern regions of the United States (Ball 1917; Bennett 1971).

The BLH life cycle is dependent upon temperature, rainfall, and host plant availability (Chen and Gilbertson 2016; Creamer 2020). Generally, leafhoppers can produce up to five generations per year in warmer regions and three generations in colder climates. Female leafhoppers deposit eggs within the epidermis tissue of the leaf or stem and these hatch in 5-40 days. A single mated female can lay between 200-300 eggs (Severin 1946). Once hatched, the leafhoppers will pass through five nymphal instars before reaching adulthood (Ball 1917; Douglass and Cook 1952). Infected leafhoppers do not pass down the virus to their offspring transovarially, instead nymphs acquire the virus through feeding on infected plants post-emergence (Soto and Gilbertson 2003; Bennett 1971).

The leafhopper transmits the virus in a circulative, non-propagative manner, meaning the virions circulate throughout the body of the insect but do not replicate within the insect tissues (Bennett 1971; Chen and Gilbertson 2016). Virus acquisition in BLH can occur after 1-2 minutes of feeding on infected plant phloem, however longer feeding periods results in more efficient transmission (Bennett 1971). There is a four-hour virus latent period after feeding for the virions to migrate from the insect gut through the hemolymph and into the salivary glands (Soto and Gilbertson 2003). After this time, the virus is persistent in the leafhopper and can be spread for days to weeks post feeding (Chen and Gilbertson 2016). Leafhoppers at all life stages can transmit the virus although younger adults are more efficient than older adults, and first instar nymphs are more efficient than later instars (Bennett 1962). It was also determined that males had higher transmission rates than females most likely due to females focusing on oviposition (Bennett 1962).

Leafhopper behavior and preference has been studied throughout the history of the insect. Various studies have indicated that sugar beets are the preferred host of BLH as evident by

prolong settling and feeding, high survival rates, and successful reproduction (Thomas 1972; Thomas and Boll 1977; Munyaneza and Upton 2005). In cafeteria-style choice feeding assays, 94% of leafhoppers from California preferred to feed on sugar beet, while 84% of New Mexico leafhoppers preferred to feed on kochia, a known weed host (Hudson et al. 2010). Further experimentation found that although BLH is able to feed upon plants such as chili pepper, tomato, and dry bean, they are not able to survive or reproduce on these plants (Hudson et al. 2010; Munyaneza and Upton 2005).

BCTV epidemiology

Epidemiology of BCTV is dependent upon many factors such as climate, plant diversity, cropping cycles, and most importantly, the presence of the beet leafhopper (Creamer 2020). BLH migrate annually from overwintering sites within the western regions of the U.S. and into agricultural fields. Several factors influence BLH movement into a region including climate, host plant availability, and leafhopper reproduction (Figure 3) (Creamer 2020; Horton et al. 2018). A classic example, is in New Mexico where BLH overwinter in annual winter weed species such as London rocket (*Sisymbrium irio* L.) and Kochia (*Kochia scoparia* L.) (Creamer 2020). In the spring, leafhopper populations rise, and broods will move into newly planted agricultural fields once weed species begin to dry down. Similar migration patterns are found in California, where leafhoppers overwinter in the foothills of the Coastal Range on winter annual weeds. In the late spring and early summer, seasonal rainfall decreases and these weed species dry down, leading to the migration of the leafhoppers into the irrigated agricultural valley in search of new host plants (Bennett 1971). Leafhopper populations are traditionally monitored throughout the growing season using yellow sticky cards, and insect traps to assess population dynamics and determine when management efforts should be implemented.

Disease management

Effective management strategies used to control curly top disease mostly focus on prevention through cultural controls, chemical control, and planting resistant cultivars. Cultural controls are effective preventative techniques for reducing leafhopper populations and virus inoculum in the landscape. These practices include removing BCTV-infected plants and any surrounding weeds that can serve as virus reservoirs. Some growers may opt for earlier crop planting dates as it has been proven that younger plants are more susceptible than older plants (Wintermantel and Kaffka 2006). Early planting allows for young seedlings to become established and thus more tolerant if infected. The use of mulches and plastic barriers have also been investigated as a deterrent for BLH landing on or near plants with mixed evidence. Reflective mulches have shown to prevent insects from feeding on plants without restricting plant growth, however, some trials found no benefit from mulch or plastic barriers (Sarwar 2020; Creamer 2020).

Chemical control offers the most effective protection against leafhoppers and potentially decreases the spread of the virus. Neonicotinoids and pyrethroid sprays are the most commonly used pesticides for controlling leafhoppers in sugar beet production. Neonicotinoid pre-emergent seed treatment is a systemic insecticide that protects the young seedlings for up to 60 days (Strausbaugh et al. 2014, 2016). However, neonicotinoids have faced recent global scrutiny for their negative effects on pollinators, birds, and surrounding aquatic wildlife, therefore, there is a need to evaluate other control strategies (Wood and Goulson 2017). Pyrethroid sprays have been implemented as a means of midseason control of leafhoppers after seed treatments have worn off (Strausbaugh et al. 2014). Nevertheless, there will always be negative effects associated with

chemical control such as increased associated cost, human and environmental safety risks, and the potential for resistance to build within pest populations.

Sugar beet breeding programs were started in the early 1900's to develop BCTV resistant cultivars. Early resistance was found in Middle Eastern sugar beet varieties and crossed with breeding lines adapted for growing conditions in the U.S. (Chen and Gilbertson 2016). Resistant cultivars can be used as a means of control; however, most varieties exhibit low to moderate resistance to BCTV. While these varieties have reduced symptoms when infected, there has been a documented yield tradeoff in which uninfected plants have reduced yield compared to susceptible varieties (Kaffka et al. 2002). Given the yield tradeoff, these varieties are typically only used in fields with high BLH pressure and virus incidence in previous years. In other cropping systems, BCTV resistant varieties have been identified. For common bean, a single dominate gene, Bct, was found to confer resistance to curly top disease (Miklas et al. 2009). For tomatoes and peppers, a few tolerant or resistant varieties have been identified, although the mechanism is uncertain (Bosland and Strausbaugh 2010; Sedano et al. 2012). Choice feeding assessments using Saladmaster tomato and NuMex Las Cruces pepper resistant varieties indicated that BLH did not prefer to feed on either of these varieties, yet the virus was able to be transmitted to both (Sedano et al. 2012).

Mechanisms of plant defense to viral pathogens

Plants have evolved an extensive defense mechanism that they use against invading pathogens, including viruses. These multifaceted defense systems involve many cellular processes, pathways, and protein interactions to activate and control various defense responses to virus infection. Numerous defense strategies used by plants specifically against viruses have been well documented (Wu et al. 2019; Gupta et al. 2021). Among these are general plant

defense systems such as activation of pattern triggered immunity (PTI) and effector triggered immunity (ETI) including the plant hypersensitive response (HR), as well as plant antiviral mechanisms like transcriptional gene silencing (TGS), post transcriptional gene silencing (PTGS), post-translational protein modifications, and finally hormone production (Gupta et al. 2021).

Pattern triggered immunity (PTI) and effector triggered immunity (ETI) are two plant defense mechanisms activated by distinct pathogen recognition processes. PTI provides broad pathogen defense and triggers responses such as reactive oxygen species (ROS) production, mitogen-activated protein kinases (MAPKs) activation, and the induction of defense genes. ETI is a more specific response activated by recognition of pathogen effectors through resistance (R) genes. ETI yields a stronger response than PTI, as characterized by rapid cell death through the plant hypersensitive response (HR) to prevent the spread of the invading pathogen. HR is accomplished through ROS production and changes in ion concentrations resulting in cell death (Morel and Dangl 1997).

Transcriptional gene silencing in response to geminivirus infection occurs in the nucleus when viral mini-chromosomes form (Abouzid et al. 1988). The RNA-directed DNA methylation (RdDM) pathway targets the virus and suppresses gene transcription. However, geminiviruses have encoded suppressors that counteract TGS (Wang et al. 2019). Post-transcriptional gene silencing, a process similar to RNA interference (RNAi), is one of the most notorious plant defense mechanisms. Initially, the virus is recognized by the host plant as an invading pathogen which the plant sets out to degrade. Dicer-like enzymes are used to cleave the viral RNA into small fragments. The cleaved fragments are used by the polyprotein RNA-induced silencing complex (RISCs), which seeks out matching sequences for degradation, thus actively degrading

virus RNAs. Similarly, plants may use microRNAs (miRNAs) derived from the hairpin structure found in geminiviruses to serve as templates in the RISC complex (Liu et al. 2017).

Post-translational protein modifications, including phosphorylation and ubiquitination, play a critical role in the plant response to geminivirus infection. Protein kinase enzymes interact with and phosphorylate viral proteins, hindering infection, as well as, initiate defense signaling cascades (Santos et al. 2009; Hu et al. 2019; Shen et al. 2011). Ubiquitination of proteins, another post-translational modification, is essential for protein degradation. There are three enzymes, ubiquitin-activating enzyme (E1), ubiquitin-conjugating enzyme (E2), and E3 ubiquitin ligase (E3) that are responsible for the ubiquitination process. Studies have shown that ubiquitination of geminivirus proteins is responsible for reduced symptoms of infected plants (Shen et al. 2016).

Finally, hormones play a critical role in plant defense against pathogens including viruses. The most common hormones associated with plant-virus interactions are salicylic acid (SA), jasmonic acid (JA), ethylene (ET), abscisic acid (ABA), and auxins (Santner and Estelle 2009; Pieterse et al. 2012). Cross talk and interplay of these hormones have been studied for decades and continue to help piece together plant responses to virus infection. SA and JA are known to act antagonistically of one another, while JA and ethylene are synergistic hormones (Bari and Jones 2009; Alazem and Lin 2014). JA has been known for its defense against necrotrophic pathogens and insect feeding, and has an important role in virus interactions as well (Zhang et al. 2017). Specifically for BCTV, a research group found that plants treated with a JA derivative before virus inoculation, decreased virus titer in these plants (Lozano-Durán et al. 2011). ABA, which usually regulates plant growth, has been of interest for its newly discovered role during plant-virus interactions. For most systems, ABA production is increased following

virus infection and sprayable ABA induced resistance prior to infection (Fraser and Whenham 1989; Alazem et al. 2014; Iriti and Faoro 2008). Auxins are involved in signaling for plant growth and development. In plant-virus interactions, manipulation of auxin signaling by the virus has been shown to promote replication, movement and symptom development in the plant (Müllender et al. 2021). Overall, plant hormones are a significant part of plant defense systems and understanding response mechanisms.

Tolerance mechanisms to plant viruses are understudied and thus less understood. Tolerance in cropping systems is defined as little or no impact to yield and vigor, or a reduction in symptoms of a plant while maintaining normal pathogen load (Cooper 1983). Tolerant plants have established a balance of activating plant defense responses without a significant growth trade off. While tolerant plants are not the same as resistant plants, some of the underlying mechanisms as listed above do overlap (Pagán and García-Arenal 2018). One mechanism that is unique to tolerance is adaptive resource allocation and life-history modifications to overcome potential negative consequences of infection (Pagán and García-Arenal 2020). Although understanding of tolerance is limited, there is great potential for more research in this area.

Mechanisms of plant resistance to insects

Host plant resistance to insects has been documented in many systems, most notably through host selection and host suitability (Smith 2005). Host selection is when the insects show preference for one plant variety over another, while host suitability is defined as the insect's ability to survive and reproduce on a particular variety (Painter 1951; Kogan and Ortman 1978). Insects can serve as vectors for plant-to-plant virus movement and are an integral part of virus spread. If a host plant is not preferred or suitable for the insect, virus spread in the landscape will be effected (Mauck 2016). Host plant resistance may also impact the insect's ability to acquire

and spread the virus. For example, in whitefly vectored geminiviruses, resistant varieties of tomatoes have been shown to reduce virus spread by reducing virus accumulation in the plant, and when the whitefly feeds, the virus is not able to be acquired (Lapidot and Friedmann 2002). Thus, it is evident that the complexity of virus-vector-host plant interactions cannot be studied independently, and all components must be taken into account together.

Identification of virus resistance in sugar beet

For sugar beets, annual field trials conducted by the USDA are used to screen multiple genotypes for innate resistance to BCTV dating back to the early 1930's (Carsner 1933). There are few genotypes that exhibit low to moderate resistant against the virus, and one genotype, KDH13 identified as being fully resistant (Strausbaugh et al. 2017; Eujayl et al. 2016). The underlying mechanism of resistance is unknown for these genotypes. The sugar beet genotypes used in this study were selected for further investigation based on differences in symptom severity after BCTV infection (Dorn et al. 2021). In field conditions the susceptible genotype, FC709-2, had high foliar disease ratings indicating increased symptoms and no resistance to the virus. In the same field trial, C869 demonstrated reduced symptomology and was statistically aligned with the resistant check, therefore, it was determined to have some type of resistance to the virus. EL10 is of single seed descent from self-pollinating sugar beet C869 over a six year period (McGrath et al. 2023). EL10 has been subjected to long and short read sequencing for genome assembly and is currently used as the sugar beet reference genome (McGrath et al. 2023). To better understand the underlying resistance mechanism of this genotype, it was selected for use in this study.

Research on transcriptional changes in sugar beet is primarily limited to abiotic factors. Previous research has reported global changes for sugar beet in response to low temperatures,

drought stress, and salt stress (Moliterni et al. 2015; Gutschker et al. 2022; Zou et al. 2020, 2023). There is one study that analyzed sugar beet response to beet necrotic yellow vein virus and beet soil-borne mosaic virus infection (Fernando Gil et al. 2020). Another study was conducted to identify the role of small non-coding RNAs in sugar beet against BCTV, where it was concluded that in resistant sugar beet genotypes there was an increase in plant derived micro RNAs targeting the virus capsid protein and replication related genes (Majumdar et al. 2022). However, there is a lack of research investigating the global transcriptional changes for sugar beets in response to beet curly top virus infection.

Goals and objectives

Overall, the goal of this study was to determine the mechanism of resistance in sugar beet to beet curly top virus and identify genes conferring resistance or tolerance. The specific objectives were to classify the nature of BCTV resistance in two genotypes, EL10 and FC709-2 using host suitability and host preference insect assays, and assessing viral load for each genotype, as well as characterize the global transcriptional response to BCTV infection using RNA sequencing. The guiding hypothesis was that there would be evidence of unique gene signatures in EL10 which provide an advantage to either preventing or tolerating BCTV infection.

MATERIALS AND METHODS

Sugar beet planting and growing conditions

The USDA-ARS sugar beet research unit in Fort Collins, Colorado, provided two genotypes (breeding lines) of sugar beet seeds. EL10 is a genetically inbred line derived from single seed descent over several generations of C869, which has demonstrated resistance to BCTV infection during field trials (Dorn et al. 2021). FC709-2, on the other hand, was found to be susceptible to the virus and therefore used as the susceptible control for comparison.

Sugar beet seeds were sowed directly into Pro-Mix HP+ mycorrhizae soil within 4-inch pots. Two seeds per pot were planted and thinned to one seedling post-germination. Seedlings were maintained in a growth chamber under the following conditions: 28°C (day)/21°C(night), 16h light/8h dark photoperiod. Plants remained in the growth chamber for around 25 days, until the 3-4 true leaf stage. Plants were fertilized every other week using Peters Blue 20-20-20 N:P:K fertilizer (JR Peters Inc., Allentown, PA) at the recommended dosage.

Beet leafhopper colony maintenance

Beet leafhoppers were collected from an Idaho field site and transported to Colorado State University to establish colonies. Colonies of uninfected leafhoppers and leafhoppers infected with BCTV were reared on sugar beet line BPA9000 and housed within rectangular thrips-proof mesh cages (Bioquip, Rancho Domingues, California). Leafhoppers infected with BCTV carried the Colorado/Worland strain, while uninfected colonies remained virus free. Monthly testing of plants and ten individual leafhoppers per colony was performed through routine DNA extraction and PCR testing to confirm the virus status.

DNA extraction and end-point PCR analysis

Plant DNA was extracted from sugar beet leaf tissue using the Wizard Genomic DNA Purification Kit (Promega, Madison, Wisconsin) following the plant tissue protocol. Briefly, leaf tissue was homogenized by adding two 3mm metal beads into the 2 mL collection tube and placing them in a Qiagen Tissuelyser II for 1 minute. Cells were lysed by adding 600 µl of nuclei lysis solution and incubated at 65°C for 15 minutes. Next, 200 µl of protein precipitation solution was added, and tubes were vortexed and centrifuged. The supernatant was transferred into a clean 1.5 mL tube, and DNA was precipitated using 100% isopropanol. All following centrifugation wash steps were done at 16,000g for 3 minutes. The samples were eluted in 50 µl of nuclease-free water. Extracted DNA concentration and purity were assessed using a NanoDrop One spectrophotometer (ThermoFisher, Waltham, Massachusetts) and stored at -20°C.

BCTV in the extracted leaf tissue was detected by end-point PCR using a universal BCTV primer set targeting the coat protein (Strausbaugh et al. 2017). For this primer set, the forward sequence is 'GTGGATCAATTTCCAGACAATTATC', and the reverse sequence is 'CCCATAAGAGCCATATCAAACTTC'. The reaction conditions were 10 µl DreamTaq Green PCR Master Mix (Thermo Fisher), 1 µl of the forward and reverse primers, 7 µl of nuclease-free water, and 2 µl of diluted sample DNA. All sample DNA was diluted to 50 ng/µl for virus detection PCR. Thermocycling conditions were 95°C initial denature for 5 minutes, 40 cycles of denaturation at 95°C for 1 minute, 58°C annealing for 1 minute, and 72°C extension for 1 minute, followed by a 72°C final extension for 5 minutes. The PCR products were visualized on a 1% agarose gel run at 100 volts for 25 minutes.

Beet leafhopper host suitability assay

Sugar beets at the 3-4 leaf stage were used to determine leafhopper survival and fecundity. A plant of either genotype was placed into a mesh 12” cube cage (BioQuip) within a light and temperature-controlled room. Adult leafhoppers were aspirated from the colony and sexed under a dissecting microscope. Four female and two male leafhoppers were sorted into each collection tube for placement. The insects were released onto the plant inside the cage. The number of surviving adult leafhoppers and the number of nymphs were counted once a week for three weeks. Assays were repeated twenty times with uninfected and virus-infected leafhoppers for each plant genotype.

The data were statistically analyzed using Minitab software (Minitab LLC, version 21.4.0). Separate generalized mixed models were created to analyze the average number of adult survival and nymphs at week three. Each model was analyzed using a two-way ANOVA to test interactions between plant genotype and insect virus status. A statistical difference was supported by a p-value < 0.05 for all tests.

Beet leafhopper host preference assay

Sugar beets at the 3-4 leaf stage were used for choice assays. Two plants, one of each genotype, were placed in a mesh 12” cube cage diagonally from one another. The plant's position in the cage was randomly determined. Ten adult beet leafhoppers were aspirated from the insect colony and starved for two hours before placing them between the plants. Adult insects were allowed to move freely around the cage and between plants. Counts were taken by visual observation of settled leafhoppers at 1, 2, 4, 6, 12, 24, 36, and 48 hours post-release. The assay was conducted with uninfected and virus-infected leafhoppers and replicated twenty times each.

Statistical analysis was conducted using R studio statistical software (R-Core Team 2021, Version 4.2.2). The data did not meet the assumption of normality, therefore non-parametric tests were used. Analysis was broken down by uninfected and virus-infected insects, and a Friedman test was used for the overall model, while the Mann-Whitney U test was done for individual time points. A statistical difference was supported by a p-value < 0.05.

Quantifying viral coat protein copy number in two sugar beet genotypes over time:

Virus inoculation and leaf tissue collection

Sugar beets from both genotypes at the 3-4 leaf stage were infected to determine the number of viral coat protein copies in the new growth over time. Inoculations were done by placing six virus-infected adult leafhoppers in a foam clip cage. Insects were clipped to one leaf per plant for 48 hours and then removed.

Leaf tissue was collected at 1, 7, and 14 days post-insect removal. Two leaf discs per plant were taken using a paper hole punch from the newest growth and placed in a 1.5 mL tube. The hole punch was disinfected with 10% bleach between each plant. Samples were stored at -80°C until DNA extraction and qPCR.

Quantitative PCR

Total DNA was extracted as previously described and diluted to a standardized concentration of 50 ng/µl for virus detection and quantification. Samples were tested in duplicate using a Quant Studio 3 Real-Time PCR Machine (Thermo Scientific). A qPCR primer set targeting a 106 bp coat protein segment, was optimized for this experiment. The forward primer sequence is ‘GGCTCCTTCAATGCCAAATTAC’, and the reverse primer sequence is ‘CCTTCACGTCTTCATACTTCCC’. Reaction conditions were 10 µl IQSYBR mix (Bio-Rad, Hercules, California), 0.6 µl of each of the forward and reverse primers, 7.8 µl nuclease-free

water, and 1 µl DNA. qPCR parameters were 95°C for 3:30 minutes, followed by 40 cycles of 95°C for 15 seconds, 60°C for 45 seconds, and a final melt curve of 95°C for 15 seconds, 60°C for 1 minute and 95°C for 15 seconds. Cycle quantification (Cq) values and melt curves were used to determine the number of positive samples.

A six-point standard curve was generated by creating a tenfold dilution series of an extracted bacteria plasmid carrying BCTV. The standard curve equation of $y = 3.56x + 42.82$ was used to determine the primer efficiency and virus quantification. Unknown copy numbers of the virus coat protein were determined by the equation $10^{Cq-Y/Slope}$ and log transformed. The average number of coat protein copies was determined for each genotype at 1, 7, and 14 dpi.

Statistical analysis was conducted using R Studio (R-Core Team 2021, Version 4.2.2). Since the data did not meet the assumption of normality, a Mann-Whitney U test was used to test for a statistical difference at each time point.

RNA Sequencing:

Plant growth, treatment, and sample collection

RNA sequencing experiments were conducted using a factorial design involving 2 sugar beet genotypes × 2 treatments (uninfected leafhoppers and BCTV-infected leafhoppers) × 3 timepoints (1, 7, 14 dpi) × 3 biological replicates (Figure 4). Each treatment group consisted of 3-4 individual plants per collection timepoint. Plants were grown under controlled growth chamber conditions until the 3-4 leaf stage, where they were randomized by treatment and collection timepoint within small 12” mesh cube cages. Six mixed-life stage leafhoppers from either the uninfected or virus-infected colony were clip-caged onto a single leaf. After 48 hours, all clip cages were removed, and the insects were aspirated.

Leaf samples were taken from individual plants at 1, 7, and 14 days post insect removal. The newly formed leaf was removed, split in half, and placed into two separate 2 mL tubes for RNA and DNA extraction. Samples were flash-frozen in liquid nitrogen and stored at -80°C until nucleic acid extraction. All plants were maintained to observe disease progression and symptom development for 3 weeks post-sampling.

DNA and RNA extraction and virus presence-absence testing

Individual plants were tested to confirm plant virus status at the sampling date and 3 weeks post-inoculation by endpoint PCR. DNA was extracted, and PCR tested using the methods described previously. Plants fed on by virus-infected insects were confirmed BCTV positive by PCR before subsequent RNA extraction.

Total plant RNA was extracted using RNeasy Plant Mini RNA extraction kits (Qiagen) according to the manufacturer's protocol. Frozen plant tissue was ground into a fine powder using a plastic pestle within the collection tube. Then, 450 µl of RLT buffer containing BME was added and vortexed to lyse cells. The homogenized mixture was transferred to a QIAshredder spin column, centrifuged, and the supernatant was mixed with 100% ethanol. The mixture was moved to a RNeasy Mini spin column and washed per protocol. Centrifugation steps were conducted at 10,000g for 1 minute. Final off-column RNA elution was done using 30-35 µl nuclease-free water in a new 1.5 mL tube. Total RNA purity was checked using a Nanodrop One Spectrophotometer (Thermo Fisher).

DNase treatment, qubit quantification, and RNA pooling

Total RNA was subjected to DNase treatment using a Turbo DNase kit (Thermo Fisher) to remove any genomic DNA contamination before downstream sequencing. DNase reactions included 1.5 µl DNase enzyme, 2.5 µl turbo DNase buffer, 21 µl nuclease-free water, and 4 mg

total RNA. Samples were placed on a heat block for 30 minutes at 37°C. Then, 2.5 µl of inactivation solution was added and mixed well. The tubes were centrifuged at 10,000g for 2 minutes, and the supernatant was moved to a final 1.5 mL tube.

DNase-treated RNA samples were evaluated using a Qubit 4 Fluorometer (Thermo Fisher) for RNA and DNA concentrations. The final Qubit RNA concentrations were used to evenly pool RNA samples together based on experimental design units and replicates. In total, 36 tubes of pooled RNA were created by combining 200ng of RNA from three individual plants into a single tube. Final RNA pools were sent to Novogene for strand-specific mRNA sequencing.

Library preparation

Directional (stranded) mRNA library prep was performed by Novogene using NEB Ultra II RNAseq stranded kit (New England Biolabs, Ipswich, Massachusetts). Library quality was checked using a Bioanalyzer (Agilent, Santa Clara, California), and then individual libraries were subjected to 150bp paired-end sequencing on a NovaSeq6000 (Illumina, San Diego, California).

Bioinformatic analysis of mRNA reads:

Trimming reads

Fastq files containing raw reads were downloaded from the Novogene platform and uploaded into CLC Genomics Workbench (Qiagen, Version 23.0.2). All subsequent steps were conducted using the tools within the CLC program and default parameters were used for each step unless otherwise noted. Raw reads were trimmed to remove sequencing adaptors, poly-N regions, and low-quality reads using a cut off Phred-score <20.

Mapping to reference genome

The EL10 sugar beet reference genome (version EL10.2_2) was downloaded from the Phytozome repository and uploaded into CLC Genomics Workbench (https://phytozome-next.jgi.doe.gov/info/Bvulgarisssp_vulgaris_EL10_2_2). Using the "map reads to reference" tool, the trimmed reads from each genotype were individually mapped to the reference genome with no masking selected. Read count files at the gene and transcript levels were produced and standardized in transcripts per million (TPM) for further analysis. Principal component analysis plots (PCA) were generated using the 36 read count files to show the clustering of samples. The PCA plot created led to the decision to make treatment comparisons within each genotype rather than comparing one genotype to the other.

Differential expression analysis

Differential expression analysis was conducted using the default settings on normalized transcript level count files. Comparisons of virus infected BLH feeding (BCTV-inoculated) to uninfected BLH feeding (mock-inoculated) at each time point for both genotypes were used to generate three comparisons per genotype. For each comparison, the transcripts were filtered by a log2 fold change >|1| and a false discovery rate (FDR) p-value < 0.05 to qualify as differentially expressed.

Functional analysis and gene ontology

Omics Box software (BioBam, Version 3.0.29) was used for functional analysis and gene ontology of differentially expressed transcripts (DETs). Each DET was scanned through NCBI BLAST and assigned a gene ontology (GO) annotation, description, and function. GO terms were assessed and compiled into like groups for biological, molecular, and cellular processes. Gene Set Enrichment Analysis (GSEA) was conducted on individual comparisons, but no further

analysis was sufficient due to a low number of DETs. Omics Box Interpro scan analysis of protein domains and motifs was conducted on each comparison to evaluate protein groups of interest.

Weighted Gene Co-expression Network Analysis

A weighted gene co-expression network analysis (WGCNA) was performed using R Studio statistical software (Version 4.2.2) and the WGCNA R software package to determine a pairwise relationship between sugar beet transcripts (a total of 25,325 transcripts). The log2-transformed, normalized transcripts per million (TPM) count data for each genotype was used to generate two separate data set matrixes. These matrixes were used for network construction to determine modules (clusters) of highly correlated transcripts.

The input count matrixes were generated and cleaned for excessive missing values. The samples were matched to their corresponding treatment group (mock-inoculated vs. BCTV-inoculated) and collection timepoint (day 1, day 7 or day 14). Next, the similarity of gene expression profiles was assessed using the Pearson's correlation coefficient and converted into network adjacencies using the signed network type with a soft thresholding power of 14. The consensus topological overlap was computed with a minimum module size of 30, after which the module eigengenes were calculated and clustered for each genotype. The modules sharing 75% similarity were merged using the Dynamic Tree Cut method (Supplementary Figure 3) and the eigengenes of merged modules were re-calculated. Consensus modules were identified as significantly associated with treatment group and timepoints based on Pearson's correlation coefficients and a p-value ≤ 0.05.

RESULTS

No difference in adult beet leafhopper survival or the number of nymphs produced on either sugar beet genotype

To determine the survival and fecundity of adult beet leafhoppers when reared on a single genotype, no-choice assays were conducted over a three-week period. The percentage of surviving adult leafhoppers was calculated, and the number of nymphs counted each week for both the EL10 and FC709-2 genotypes (Figure 5 A&B). In the first week, approximately 80% of adults survived on either genotype regardless of insect virus status. Week 2 had a 70% survival rate for all groups. After three weeks, the average adult leafhopper survival was around 50% when reared on either genotype regardless of insect virus status, with no statistical significance (Two-way ANOVA: Genotype (F= 0.75, df= 1, p= 0.39) and insect virus status (F=0.90, df= 1, p= 0.35)).

The mean number of nymphs was recorded each week to assess leafhopper fecundity. No nymphs had emerged for either genotype in the first week (Figure 5 C&D). By the second week, infected leafhoppers had an average of 10 nymphs, while uninfected leafhoppers had an average of 30 nymphs on either genotype. At week three, virus-infected leafhoppers reared on EL10, and FC709-2 had an average of 32 and 45 nymphs produced, respectively. In contrast, uninfected leafhoppers had an average nymph count of 86 for EL10 and 90 for FC709-2. There was no statistical difference in the fecundity of adult females when reared on either genotype; yet uninfected leafhoppers had a higher fecundity than virus-infected leafhoppers (Two-way ANOVA: Genotype (F= 3.25, df= 1, p= 0.076) and insect virus status (F= 12.4, df= 1, p= 0.001)).

Virus-infected leafhoppers prefer to settle on the susceptible genotype rather than the resistant

To assess whether host plant genotype influenced leafhopper settling preference, adult leafhoppers were presented with a choice between the two genotypes, and their behavior was monitored over 48 hours (Figure 6). Overall, uninfected leafhoppers showed no clear preference; however, they did have a statistically significant preference for the susceptible genotype at 24 and 48 h (Supplementary Table 1). Virus-infected leafhoppers strongly preferred to settle on the susceptible genotype, FC709-2, starting at 4 h, and once the choice was made, the virus-infected leafhoppers did not move from the susceptible genotype over the duration of the experiment (Supplementary Table 1).

Quantification of BCTV viral load show no difference between genotypes

To evaluate the average BCTV copy number within infected sugar beets across different time points, absolute quantification of the virus coat protein was determined by generating a reliable standard curve of a plasmid containing the BCTV coat protein. The Cq values for each standard were plotted against the known copy number of the plasmid, resulting in a six-point standard curve graph ranging from 1.7×10^8 to 1.7×10^3 BCTV coat protein copies (Supplementary Figure 1). The calculated correlation coefficient (R^2) for the standard curve was 0.9993, while the primer efficiency was calculated to be 91% and the melt curve analysis showed a specific melting temperature of 80°C.

Amplification signals were consistently detected in both genotypes at all time points confirming the presence of the virus. Notably, the day 1 timepoint had the lowest number of virus particles with EL10 averaging 9.3×10^4 copies and FC709-2 averaging 7.4×10^2 copies, while day 14 had the highest averages of 1.9×10^8 for EL10 and 6.3×10^8 for FC709-2 (Figure

7). As time progressed, there was a consistent upward trend in virus copy numbers for each genotype indicating active replication is occurring. However, there was no statistical difference in means observed between the genotypes on day 1 (p-value = 0.67), day 7 (p-value = 0.69) or day 14 (p-value = 0.78).

Infected sugar beets at 3 weeks showed differences in symptom severity (Figure 8). FC709-2, the susceptible genotype, showed classic BCTV symptoms including severe curling, rugosity, and crinkling of leaves. Alternatively, EL10 had enlarged veins on the underside of the leaf but the curling of the leaves was less severe and overall, the plants were less symptomatic. Reduced symptoms while maintaining similar viral loads indicate that EL10 is possibly tolerant to virus infection.

RNA sequencing to investigate transcriptional responses to BCTV in EL10 and FC709-2

Quality control of raw reads

Thirty-six RNA-sequencing libraries made from mock-inoculated and BCTV-inoculated sugar beets from each genotype passed initial quality control checks to be sequenced. Returned RNA-seq libraries had a minimum of 6 gigabases (GB) of data per library. Post-read trimming and filtering, there was an average of 44.1 million read pairs per library, with the highest outlier having 83.0 million reads and the lowest being 32.0 million reads (Table 1). The average percentage of reads with a Phred score >20 was 92% with a slight variation of ±4%. All samples were mapped to the EL10 reference genome where the average number of reads mapped was 38.1 million reads, or 86% of cleaned reads. There was no significant difference between the number of reads that were mapped from the EL10 libraries and the FC709-2 libraries (students t-test, p-value = .991).

A principal component analysis (PCA) plot using mapped transcript reads (Figure 9) showed strong clusters for each genotype with no overlap, suggesting significant differences in their gene expression profiles. Within each genotype cluster, there is grouping by time point. The early timepoint, day 1, tends to fall near the bottom of the groups while later timepoints of day 7 and 14 lie near the top. Given the strong clustering by genotype, it was noted that the two sugar beet genotypes used are genetically different, and therefore comparing them to one another would result in false differences related to plant genotypes rather than the response to virus infection.

Differentially expressed transcripts identified for each genotype at three time points

Comparisons of mock-inoculated vs. BCTV-inoculated plants at each time point for both genotypes were made, resulting in 6 lists of differentially expressed transcripts (2 genotypes x 3 time points). A total of 25,326 genes were statistically analyzed for differential expression, of which, transcripts with an FDR p-value < 0.05 and a logfold2 change greater than |1| were considered to be differentially expressed. For each comparison, we created lists of the top 30 upregulated and downregulated transcripts (Tables 2-7).

To visualize differentially expressed transcripts (DETs), volcano plots were generated for each genotype at the three time points (Figure 10). For EL10, on day 1, there were 40 DETs, on day 7, there were 40 DETs, and 30 DETs on day 14. In FC709-2, on day 1, there were 53 DETs, day 7 had 62 DETs, and day 14 had 323 DETs. Overall, in EL10, the number of DETs stayed the same or decreased over time, while FC709-2 had an increase of DETs at each time point. Notably, EL10 had fewer DETs expressed at each time point than FC709-2. Among both genotypes, there was an equal balance of upregulated and downregulated DETs, except for FC709-2 on day 14, where there were 6x more upregulated DETs than downregulated.

To determine the overlap in the two sugar beet genotypes' response to the virus, an upset plot was created (Figure 11). Within EL10, there were few shared DETs between the time points and no DETs that overlapped all three time points. There was one mutual DET, choline kinase 2, upregulated on both days 1 and 7. Between day 1 and 14, there was a single shared DET of histone acetyltransferase HAC1, that was upregulated at first and then downregulated. There were three mutual DETs between days 7 and 14: protein DDB_G0276689 and photoconvertible water-soluble chlorophyll-binding protein were upregulated, while the regulator of nonsense transcripts 2 protein was downregulated.

More overlap was found in FC709-2 response to virus infection over time. All three timepoints shared tuftelin-interacting protein 11, which was downregulated until day 14 when it was found to be upregulated. For FC709-2, between days 1 and 7 there were 4 DETs in common; between days 1 and 14, there were 5 DETs, and between days 7 and 14 there were 12 DETs.

In comparing EL10 to FC709-2, there was minimal overlap for each time point. On day 1 there were three shared DETs of protein LNK1-like isoform, receptor protein kinase TMK1, and protein SCAR2 isoform X1. On day 7, there was one DET in common and that was benzyl alcohol O-benzoyltransferase. For day 14, there were three shared DETs of tyrosine phosphatase, conserved oligomeric Golgi complex subunit 4, and basic endochitinase. The absence of more commonly shared DETs reinforces the distinct response to virus infection of each sugar beet genotype.

Gene ontology terms assigned to each sugar beet genotype in response to virus infection

Gene ontology (GO) terms were assigned using Omicsbox software to each differentially expressed transcript and the sugar beet reference genome file to create a background data set. Functional analysis of these terms classified them into the following categories: biological

processes, molecular function, and cellular components. GO enrichment analysis was conducted for each list of DETs; however, there were no enriched pathways due to the limited number of DETs. Enriched pathways were only found for FC709-2 on day 14.

The number of differentially expressed terms for each GO category showing changes in the plant response over time were determined (Figures 12 & 13; Supplementary Figure 2). Biological terms for each genotype included plant response to stimulus, metabolic processes (primary metabolic process, organic substance metabolic process, cellular metabolic process, and nitrogen compound metabolic process), and immune response (Figure 12A & 13A). For each category there was a significantly smaller number of terms identified in EL10 as compared to FC709-2. For response to stimulus at day 1, EL10 had twice as many upregulated terms than FC709-2. However, on day 14, FC709-2 had upregulated nearly 20x as many response to stimulus genes. Terms relating to the plant metabolic processes were primarily upregulated at day 1 for EL10 and FC709-2 yet changed as time progressed. On day 7 and 14, EL10 had downregulated 59% and 76%, respectively, of all terms related to primary metabolism. Meanwhile FC709-2 had upregulated 53% of terms on day 7, and 83% of terms on day 14 under the primary metabolism GO category. Terms relating to the plant immune response were found only on day 14 for both genotypes. EL10 had 36% of terms upregulated while FC709-2 had 100% upregulation of immune response GO terms.

Cellular GO terms were shared between the two genotypes including intracellular organelle, membrane-bounded organelle, and plasma membrane (Figure 12B & 13B). For EL10, there was a similar number of terms upregulated and downregulated on day 1 and 7 for the three categories above. Whereas FC709-2 on day 1 and 7 had a majority of downregulated genes in these categories. Interestingly, on day 14, EL10 had downregulated more than 50% of terms

relating to the intracellular organelle, membrane-bounded organelle, and plasma membrane; while FC709-2 had upregulated more than 80% of terms in these categories. The most notable is the 100% upregulation of terms related to the plasma membrane in FC709-2. The differences in cellular components, specifically at day 14, are consistent with virus infection and manipulation of the host plant for FC709-2, while EL10 does not show these modifications.

Scanning of DETs for associated protein families

The DETs for each genotype and timepoint were scanned against the InterPro database and classified into families that have similar functions and roles within the plant. Each protein family shows the number of sequences associated but does not include direction or magnitude of these terms. Protein families present at the highest levels for EL10 on day 1 include many involved in biological processes such as cell signaling, transcription and protein – protein interactions (Figure 14A). Similarly on day 1 for FC709-2 protein families related to biological processes were identified, but unique families related to terpene synthesis were only detected in this genotype (Figure 14B). Terpene related protein families included, terpene synthesis N-terminal domain superfamily, terpenoid cyclases/protein prenyltransferase, and isoprenoid synthase domain superfamily.

Moving forward to day 7, protein groups for EL10 include proteins family such as DUF538 which has been classified as a chlorophyll binding protein in stressed plants, and NAD binding domain which plays a role in pest resistance and stress response (Figure 15A). Protein families for FC709-2 include many DNA binding families and the same three terpene synthesis families identified in day 1 (Figure 15B).

Day 14 protein families of EL10 were found to include AP2/ERF domain which is responsible for ethylene production, DUF538 protein family, as well as multiple RNA and DNA

binding families (Figure 16A). FC709-2 had protein families related to biological processes, peroxidase formation, and WRKY transcription factors which are involved in regulating plant defense (Figure 16B).

Functional grouping of DETS to analyze plant response to virus infection

Further exploration of the DETs found for each genotype over time revealed groups of related transcripts that take part in various plant processes. The roles of individual transcripts within the DET tables (table 2-7) were categorized based on their role in hormone signaling, protein production and ubiquitination, cell cycling, stress reduction, and volatile synthesis. These functional groups provide context to the unique plant response to virus infection for each genotype.

Hormone Signaling

Plants recognize and defend themselves from invading pathogens through the production of specific hormone pathways. Many of these pathways play vital roles in understanding the plant defense response. In EL10, hormones associated with jasmonic acid (JA), ethylene (ET), and abscisic acid (ABA) pathways were found to be elevated at multiple timepoints (Table 2-4). In contrast, FC709-2 included DETs associated with auxin and ABA pathways, that were both up and downregulated throughout the time course (Table 5-7).

In EL10, DETs related to hormonal cross talk including suppressors of salicylic acid production, and positive regulators of ABA and ethylene synthesis were found on day 1 (Table 2). DETs within FC709-2 related to auxin hormone signaling were both up and down regulated at day 1 along with downregulated ABA related transcripts (Table 5). Day 7 DETs included positive regulation of ABA and ethylene production, as well as jasmonic acid precursors in EL10 (Table 3). FC709-2 had different expression patterns of two DETs related to the ABA pathway, one of

which was slightly upregulated and the other significantly downregulated (Table 6). There was also an increased production of the salicylic acid precursor, benzoic acid in these plants. On day 14, DETs being upregulated in EL10 were components of the ABA pathway (Table 4). DETs found in FC709-2 included one upregulated transcription factor in response to SA or JA, but notably DETs related to plant systemic acquired resistance and defense response proteins were also upregulated in this genotype and not found within EL10 (Table 7).

Protein production and protein ubiquitination

Protein production is essential to plant homeostasis and plays a large role in plant defense response to pathogens. Essential DETs linked to transcription, mRNA processing and polymerase activity were found in both plant genotypes. On day 1, both genotypes had numerous upregulated DETs with roles related to protein production (Table 2 & 5). However, on day 7, both genotypes shifted to suppression of protein production as each had twice as many downregulated DETs compared to upregulated (Table 3 & 6). On day 14, EL10's DETs related to protein production were downregulated, in contrast to FC709-2, which had a combination of both up and downregulated DETs (Table 4 & 7).

Protein ubiquitination is known to activate the plant immune response after pathogen recognition and was observed in both genotypes throughout the timepoints. On day 1, EL10 had two upregulated and one downregulated DET associated with the E3 protein ubiquitin ligase enzyme, while FC709-2 had one upregulated and two downregulated DETs (Table 2 & 5). By day 7, E3 ubiquitin DETs for EL10 included three downregulated transcripts while FC709-2 had three upregulated (Table 3 & 6). On day 14, EL10 had two upregulated transcripts and FC709-2 had one upregulated and one downregulated transcript (Table 4 & 7).

Plant growth and cell cycling

Processes related to plant growth and cell cycling were identified in both genotypes. Geminiviruses have been shown to manipulate plant host cells by inducing the cell cycle and promoting virus replication (Ascencio-Ibáñez et al. 2008). In EL10 on day 1 DETs associated with plant growth were downregulated, whereas those found in FC709-2 were upregulated. This trend is seen at day 7 as well, where two EL10 cell cycling DETs are downregulated while two FC709-2 transcripts of similar function are upregulated, and one additional DET is downregulated (Table 3 & 6). On day 14, there is only one DET for EL10 related to plant growth that is upregulated, whereas FC709-2 has twice as many upregulated cell cycling DETs than downregulated (Table 4 & 7).

Stress reduction of ROS

Reactive oxygen species (ROS) are produced by plants as a defense mechanism against invading pathogens; however, accumulation of these molecules can lead to oxidative stress. Detoxification of these molecules within the plant is important for plant survival and reduced symptom development. Transcripts known for stress reduction, such as choline kinase 2 and scarecrow like protein 14 among others, were found to be highly upregulated at day 1, day 7 and on day 14 for EL10 (Tables 2-4). In FC709-2, similar stress reduction transcripts were found to be primarily upregulated on day 1 before being heavily downregulated on day 7 (Tables 5 & 6). By day 14 in FC709-2 ROS detoxification DETs were upregulated once again (Table 7). The ability of EL10 to reduce the level of ROS accumulation and detoxify the cells at all timepoints may lead to less severe symptom development as compared to FC709-2.

Volatile production in response to insect feeding and virus infection

Plants can produce volatile organic compounds (VOCs) as environmental cues in response to insect feeding or virus infection. The VOCs released can be attractive to insect vectors or to their predators. In EL10 volatile production was found only on day 7 and being downregulated in the virus infected plants (Table 3). In contrast, FC709-2 had notable volatile production at each timepoint. There was upregulation at day 1 and 14 of the enzyme (-) germacrene D synthase, a known volatile that attracts insects to the plant for feeding (Tables 5 & 7) (Mozuraitis et al. 2002). Two other volatile synthesis enzymes were identified on day 7 for these plants. The increased volatile production in FC709-2 may lead to insects being attracted to this genotype as opposed to EL10 post inoculation.

WGCNA

The WGCNA was used to identify modules of co-expressed transcripts within the sequencing data. Overall, there were 23 clustered modules found post merging (Supplemental Figure 3). For EL10, the module thistle1, was identified as significantly correlated with the BCTV infection treatment group with a correlation coefficient of 0.39 and p-value of 0.04 (Figure 17). For FC709-2, the same module thistle1 was found to be significantly correlated with BCTV infection (correlation coefficient = 0.43 and p-value = 0.03) as well as a unique module, skyblue, that was only significant in the FC709-2 genotype (correlation coefficient = 0.38 and p-value = 0.05) (Figure 18). For the thisle1 module, 45 transcripts made up the consensus module and five considered as hubs. Included in these were genes relating to phloem development that were found to be overexpressed within this module. However, none of the transcripts identified in thisle1 were differentially expressed in EL10, and only one DET was found for FC709-2. The skyblue module contained 205 associated transcripts and 20 of which as hubs. Overexpressed

transcripts in this module were related to plant defense, specifically salicylic acid production. There were 17 hub transcripts that were found to be differentially expressed in FC709-2 and 84 DETs throughout the entire module.

DISCUSSION

Plants have evolved distinct defense systems to combat insect pests and pathogens (Zhang et al. 2023). This study aims to investigate underlying plant mechanisms of resistance in sugar beet when challenged with BCTV, and assess potential effects on the virus vector, the beet leafhopper. The findings presented shed light on the global transcriptional changes that occur post infection including altered expression of metabolic pathways and host plant defense responses between the susceptible and resistant genotype of sugar beet; as well as explore the possibility of host plant resistance to leafhoppers.

Characterizing the mechanism of resistance in plants includes conducting host suitability and preference assays that can shed light on host plant resistance to the vector. In preference assays for this study, virus-infected leafhoppers revealed a strong choice of the susceptible genotype, which could be accounted for in the differentially expressed transcripts and related to volatile production in these plants. Specifically, the upregulation of (-)-germacrene D synthase in FC709-2, which has been proven as an insect attractant to certain species (Mozuraitis et al. 2002; Abraham et al. 2014). The increase in protein families associated with volatile organic compounds (VOCs) and terpene synthesis found in FC709-2 at all timepoints further supports this finding. Therefore, it is possible that virus induced changes in plant volatile production was the cause of attraction for virus-infected leafhoppers to FC709-2, and not a mechanism found within EL10. The use of VOCs as insect attractants or deterrents have been shown to be an effective tool for use in the push-pull strategies of IPM (Cook et al. 2007). Behavior manipulation of insects using VOCs has been documented for many insect pest, including other

leafhopper species, however, more experimentation would be needed to fully comprehend VOCs and their effects on beet leafhopper (Dáder et al. 2015; Nebapure et al. 2022; Niu et al. 2022).

Virus replication within the host plant is essential for establishing infection and symptom development, yet this process may be hindered in resistant plants. For BCTV, increased virus replication and accumulation has been linked to an increase in disease severity (Wintermantel and Kaffka 2006). However, when we tested for virus accumulation in each genotype, there were similar viral loads despite differences in symptom severity where FC709-2 had more severe symptoms than EL10, which showed reduced symptoms. Considering the definition of tolerance, EL10 may be exhibiting tolerance to virus infection rather than resistance. Tolerance has previously been documented for beet yellows virus and beet western yellows virus in sugar beet, although the mechanism is not understood (Wintermantel 2005). For EL10, more studies are needed assessing yield and sugar content of infected plants to draw any final conclusions.

Several studies looking to identify transcriptional differences of resistant and susceptible plant genotypes to geminivirus infection have been conducted on tomato (Chen et al. 2013), casava (Allie et al. 2014), cotton (Zaidi et al. 2020), and melon (Sáez et al. 2022). Trends in our data set indicate similarities between the sugar beet genotypes response to geminivirus infection. Similar to previous works, there were fewer DETs associated with the resistant genotype than the susceptible at all timepoints, and minimal overlap of shared DETs between the groups. The lack of shared DETs between genotypes and timepoints indicates a dynamic response to virus infection that is unique to each genotype. This also alludes to the fact that the sugar beet genotypes used are genotypically distant and solidifies our comparisons of genotypes individually rather than against one another.

Both genotypes had a unique defense response to virus infection which changed over time. FC709-2 exhibited classic ETI response on day 1 as characterized by the activation of a probable disease resistance protein and induced hypersensitive response. Hormones relating to SA and auxin production were also upregulated in this genotype. During infection, geminiviruses C4 protein interact with host proteins to reprogram and promote auxin biosynthesis as it stimulates cell proliferation and virus pathogenicity (Zaidi et al. 2020; Vinutha et al. 2020; Jongbum et al. 2004). This is supported in FC709-2, where there was an increase in cell cycling and intensified symptoms of this genotype. Contrastingly, EL10 showed evidence of increased protein kinase activity and ROS production indicating that the defense response was activated, even though transcripts related to pathogen recognition were not identified. Pathogen recognition takes place quickly, sometimes after minutes of entry and so the day 1 timepoint was too late (Abramovitch et al. 2006; Bigeard et al. 2015). Transcripts associated with JA and ABA production were highly expressed in EL10 on day 1 which confirms activation of plant defense pathways. In EL10, the upregulation of JA most likely suppresses SA pathways because of the antagonistic relationship between the hormones, which is contradicting to most documented geminivirus infections where SA is upregulated (Ascencio-Ibáñez et al. 2008; Li et al. 2019; Zhang et al. 2023). Studies have tested priming of plants through exogenous JA sprays prior to virus inoculation and found that the treatment disrupts infection of BCTV, indicating that suppression of JA through SA activation is done by the virus to promote infection (Lozano-Durán et al. 2011). Another important factor to be considered is the effect of leafhopper feeding, which has been shown to increase JA production in plants (Cowles et al. 2018; Kallenbach et al. 2012; Sugio et al. 2011). Even so, the virus has evolved strategies to quickly counteract host hormone production as evident in FC709-2 where SA production was upregulated. Notably, the

induction of JA in EL10 suggests that the genotype is not manipulated by the virus or that it has an alternative mechanism for up-regulating JA after initial infection.

By day 7, FC709-2 exhibited ROS production and increased precursors of JA. Interestingly, specific defense related proteins like disease resistance protein RPP13 and germin-like protein were downregulated at this timepoint, which in turn would favor virus survival in the host. Whereas, EL10 increased JA and aspartate oxidase, which is responsible for ROS burst in PTI and required for stomatal immunity (Macho et al. 2012). This timepoint did not reveal much in terms of the plant defense response for EL10.

At the final timepoint of day 14, FC709-2 exhibits upregulation of transcripts associated with systemic acquired resistance (SAR) most likely due to SA production (Klessig et al. 2018). In EL10, ABA and gibberellin acid (GA) were being produced but no other defense related hormones. Production of GA can be related to the symptoms within EL10, as GA increases cell proliferation by inducing the cell cycle. Geminiviruses have been shown to manipulate the cell cycle for its own replication which leads to symptoms such as vein swelling and small tumorous growths on plant leaves (Ascencio-Ibáñez et al. 2008; Gupta et al. 2021). Since we found that the virus is able to replicate within EL10 and increases over time, it is not surprising that the virus has potentially manipulated the host to increase cell cycling. The symptoms observed in EL10 also support this theory. Overall, each plant had a significant yet distinct response to BCTV infection. FC709-2 mounted a response by increasing SA production and ultimately succumbed to infection. While EL10 primarily increased JA and ABA, both of which have been associated with resistance or tolerance in other systems (Sáez et al. 2022; Allie et al. 2014).

For plants to survive they need to maintain homeostasis by consistently regulating genes involved in biological processes and cellular homeostasis. In EL10, BCTV-inoculated plants

showed a significant downregulation of biological GO terms related to primary metabolic processes, organic substance metabolic process, cellular metabolic process and nitrogen metabolic processes as virus infection progressed. The decrease in metabolic processes is typically linked to the activation of immune response where energy and resources are redirected (Rojas et al. 2014). Reallocation of resources away from metabolic process and plant growth is also a notable sign of tolerance to virus infection (Pagán and García-Arenal 2020). In contrast, FC709-2's primary metabolic processes were increased substantially as the disease progressed to day 14, which is indicative of virus hijacking of the plants normal process in exchange for excess viral replication.

Another key pathway to highlight is the reduction of ROS after initial burst to restore and maintain cellular homeostasis. It has been shown that an increase in ROS scavenging enzymes and ROS detoxification pathways are linked to increased resistance against geminiviruses and when these pathways are knocked down, resistant genotypes become susceptible to infection (Li et al. 2019; Sharma et al. 2021). Downregulation of ROS detoxification was also proven to favor replication and cellular spread of plant viruses (Clarke et al. 2002; Sharma et al. 2021). In our study, ROS detoxification was present for both genotypes, although EL10 had greatly upregulated these transcripts at all timepoints which most likely helped alleviate plant stress and decrease symptom development. ROS detoxification was initially downregulated by FC709-2, which favors the virus for replication and movement and increases susceptibility within this genotype.

Protein families identified for EL10 and FC709-2 for day 1 were associated with plant immune response and function such as protein kinase and leucine-rich repeat domain families. Both of these protein families are needed to trigger the plant defense signaling cascades

indicating quick recognition of the invading pathogen and a fast defense response time in both genotypes. At the later timepoints, a unique protein family of unknown function DUF538 is found in EL10 yet lacking in FC709-2. This specific family has been recently described as conferring stress tolerance in plants through activation of chlorophyl degrading proteins and was found to be upregulated in drought stressed plants (Yu and Kanehara 2020; Gholizadeh 2016). The upregulation of this protein family in EL10 may contribute to reduced symptoms and aid in defense against plant stress which was not found in the susceptible genotype.

Overall, multiple factors were identified for their potential role in resistance or susceptibility to BCTV infection within each genotype and are summarized in Figure 19. For EL10, key resistance mechanisms identified included the production of phytohormones JA and ABA, along with stress reduction proteins, and overall metabolism changes that reallocated critical plant resources. On the other hand, the susceptible genotype, FC709-2, was found to induce the phytohormones SA and auxin, and continuously release specific volatile organic compounds. FC709-2 increased plant metabolic processes and cell cycling which may have resulted in increased symptoms within this genotype. The overarching comparisons of these two sugar beet genotypes showed two distinct yet different responses to BCTV infection which almost certainly supports the contrasting symptom and classifications of these genotypes.

The modules identified in the WGCNA showed one shared cluster, thisle1, which contained transcripts with like expression patterns between the two genotypes after virus infection. Interestingly, transcripts relating to phloem development were over expressed, which is supported by the observed symptoms of vein swelling in each genotype. In Arabidopsis, there is a strong correlation between phloem disruption and symptom severity (Jongbum et al. 2004). Susceptible plants show complete disruption of the phloem leading to necrosis, while less

susceptible plants show less disruption and can continue the movement of nutrients and other metabolites, resulting in less symptoms. For the two genotypes used in this study, this reasoning may support the less severe symptoms noted in the EL10, the resistant genotype, even though there was virus induced changes to the phloem. On the other hand, the skyblue module was specific to the susceptible genotype, FC709-2, and included plant defense transcripts associated with SA production. SA related DETs were found only in FC709-2 and not in EL10, which supports the uniqueness of this module to the susceptible genotype.

CONCLUSIONS AND FUTURE DIRECTIONS

Overall, the main goal of this study was to determine the mechanism of resistance of sugar beet to beet curly top virus. Evaluation of the resistant and susceptible genotype showed that each genotype had a dynamic, ever-changing, response to virus infection over time that was inherently different from one another. The resistance mechanisms found in EL10 included the expression of the phytohormones jasmonic acid and abscisic acid, reduction of plant stress, and primary metabolism resource reallocation. While in the susceptible genotype FC709-2, mechanisms found included the expression of the phytohormones salicylic acid and auxins, along with volatile organic compound production and increasing of plant metabolic processes. In conclusion, the findings of this study document global transcriptional changes in sugar beet associated with virus infection for a susceptible and resistant genotype, which can be utilized by researchers and plant breeders to fully explore host plant-virus-vector interactions and enhance mechanisms of interest.

There are several promising opportunities for future research in understanding the mechanism of resistance in sugar beet to BCTV infection and possible IPM strategies. A surprising finding in this study, which warrants further investigation, is the role of plant volatiles in attracting leafhoppers. Studies to identify the specific volatiles being released including the use of gas chromatograph- mass spectrometry could be used to determine the different volatiles produced and relative concentration levels. Once identified, the volatiles should be tested as BLH attractants or repellents using Y-tube or insect preference assays. Once assessed at the field level, these specific identified volatiles may lead to advancements in IPM strategies by

incorporating them into pheromone traps or for use as trap crops that lure BLH away from a field.

Additional studies may be needed to further investigate the resistant traits within EL10. Although there was evidence of increasing viral load within EL10 using qPCR assays with mRNA targets, there is a need to quantify virus protein levels within the new growth. Some plants may inhibit protein translation as a means of resistance, which was not thoroughly investigated in this study (Machado et al. 2017). An enzyme-linked immunosorbent assay (ELISA) could be used to assess relative quantification of viral proteins specifically the coat protein within each genotype. If proteins levels were significantly lower in EL10, the mechanism of resistance may be related to hindrance of virus translation.

To fully untangle the roles of the phytohormones produced in response to BCTV infection and their role in resistance, exogenous spray applications may be used. Phytohormones identified as possible candidates to test include jasmonic acid, abscisic acid, and salicylic acid. To understand how each phytohormone elicits the plant response, an exogenous spray would be applied to the plant prior to virus infection and then monitored for virus suppression or resistance. Phytohormone sprays could be conducted independently or in conjunction with one another to determine potential synergistic or antagonistic effects on the plant defense response.

Additionally, for the plants used in this study, it would be valuable to comprehensively assess the level of tolerance in EL10 through field studies where yield and sugar content are evaluated. It would also be of use to conduct a similar study using genotypes of sugar beet with more classic characteristics of resistance to BCTV to see what overlapping mechanisms are present. Overall, this study lays a foundation for research into sugar beet response to BCTV

infection and can be used to compare mechanisms of host plant resistance or tolerance with future findings.

FIGURES AND TABLES

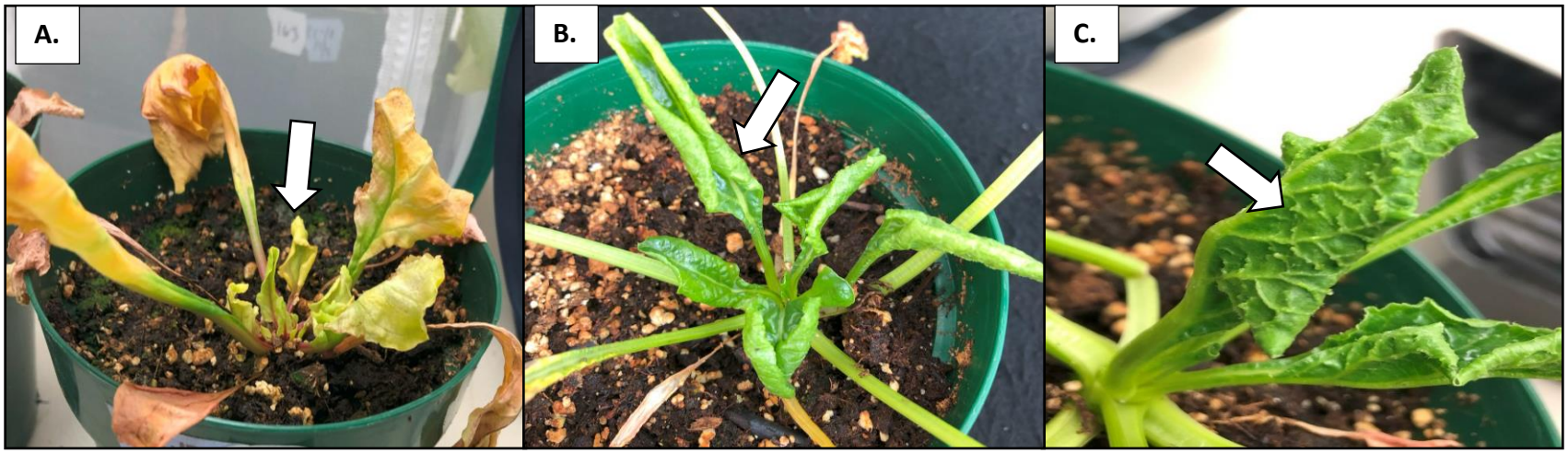

Figure 1: Symptoms of BCTV on sugar beet showing **(A)** chlorosis of the plant, **(B)** upward curling and twisting of leaves, and **(C)** thickening of the veins with small tumor like growths.

Figure 2. The beet leafhopper, *Circulifer tenellus* Baker, across different life stages. At the top is a young nymph (1-2 instar), in the middle is a late-stage nymph (3-5 instar), and at the bottom is an adult BLH. Photo credit: Max Schmidtbauer

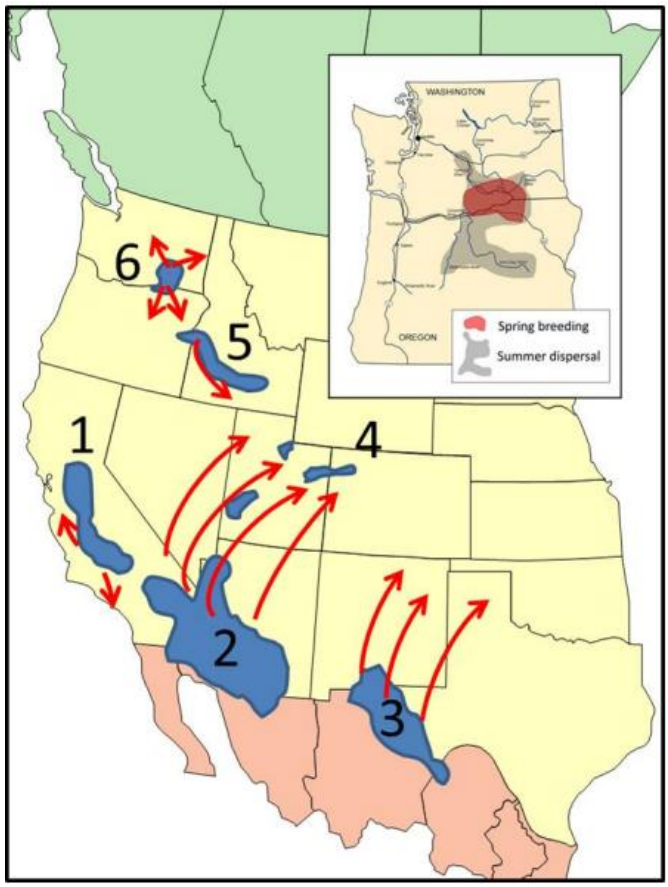

Figure 3. Migration patterns of BLH from overwintering sites (outlined in blue) to regions of agricultural production in the western U.S. (Horton et al. 2018)**.**

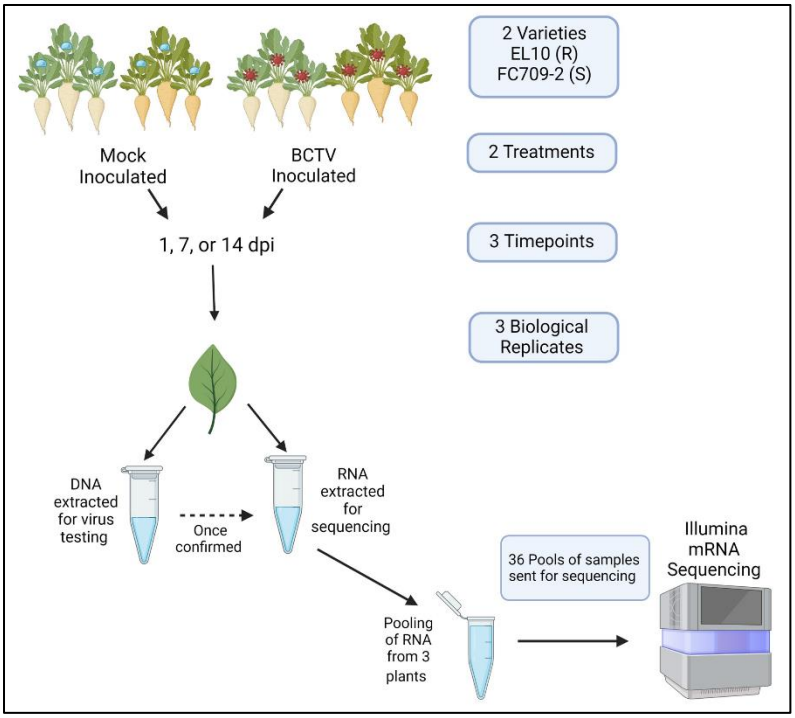

Figure 4: An overview of the RNA sequencing experimental workflow prior to being sequenced. There are two genotypes of sugar beet, EL10 and FC709-2 that will either be set with uninfected leafhoppers (mock-inoculated) or with virus-infected leafhoppers (BCTV inoculated). For each timepoint, there is a subset of 3-4 plants where the newest leaf is sampled. Each sampled leaf is divided in half and flash frozen for further testing. The DNA was extracted first to confirm the presence or absence of the virus. Once the virus status was confirmed, the RNA was extracted. Equal concentrations of RNA from three individual plants were pooled and sent for sequencing.

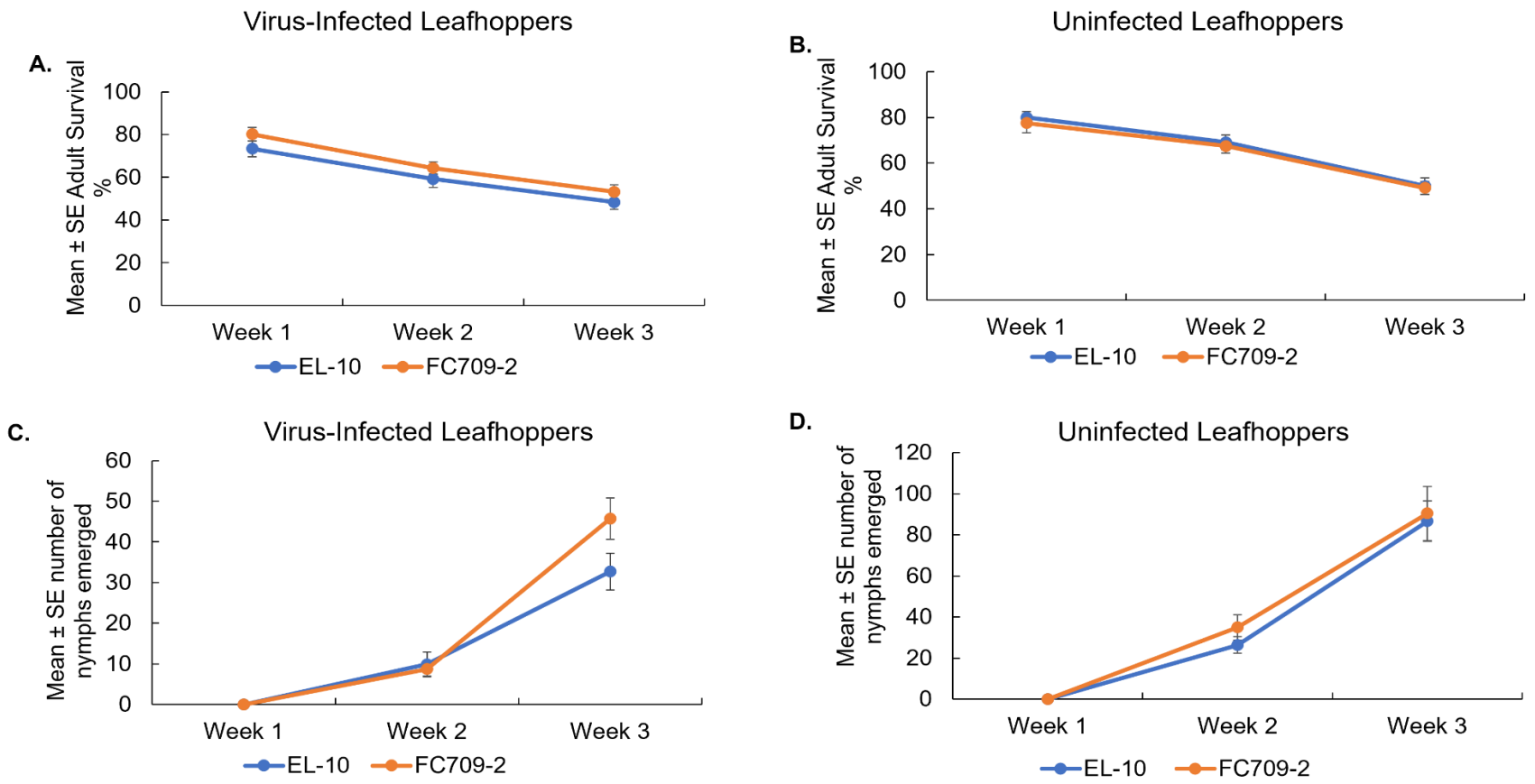

Figure 5: Average adult beet leafhopper survival and average number of nymphs emerged when reared on a single genotype of sugar beet. **(A)** Mean percent surviving virus-infected and **(B)** uninfected adult leafhoppers for each genotype over a three-week period. Each timepoint indicates the average number of surviving adults out of the six originally placed for n=20 replicates. **(C)** Mean number of nymphs counted from virus-infected and **(D)** uninfected leafhoppers on each genotype over a three-week period. Each timepoint represents the mean number of nymphs that emerged on each genotype for n=20 replicates. Statistical analysis for each was performed using a GLM by two-way ANOVA with Tukey-HSD posthoc test in which no statistical difference was determined between adult survival or nymphs produced on either genotype.

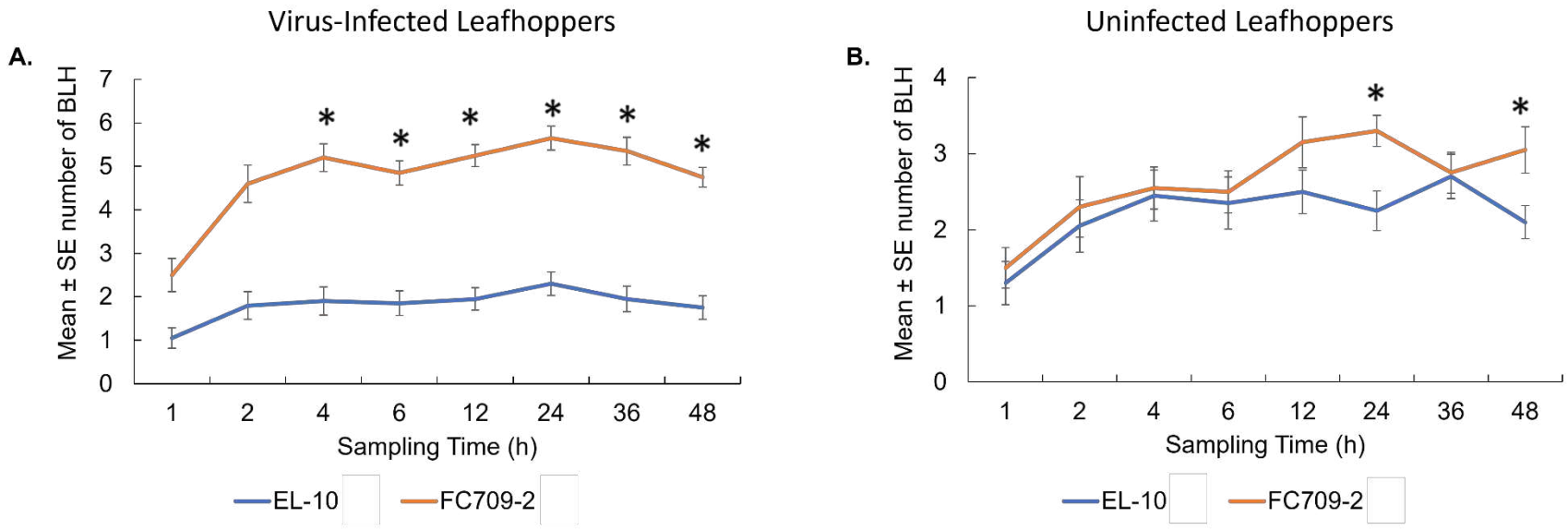

Figure 6: Settling preference of beet leafhoppers when allowed to choose between two sugar beet genotypes. **(A)** The mean number of virus-infected or **(B)** uninfected leafhoppers counted on either genotype out of the ten leafhoppers that were released into the cage. Each sampling timepoint was counted by visual observation and the mean derived for n=20 replicates. Statistical analysis was performed using both Friedman (full model) and Kruskal-Wallis (individual time points) tests, where single asterisks indicate significance at $p<0.05$. See supplementary table 1 for all statistical values.

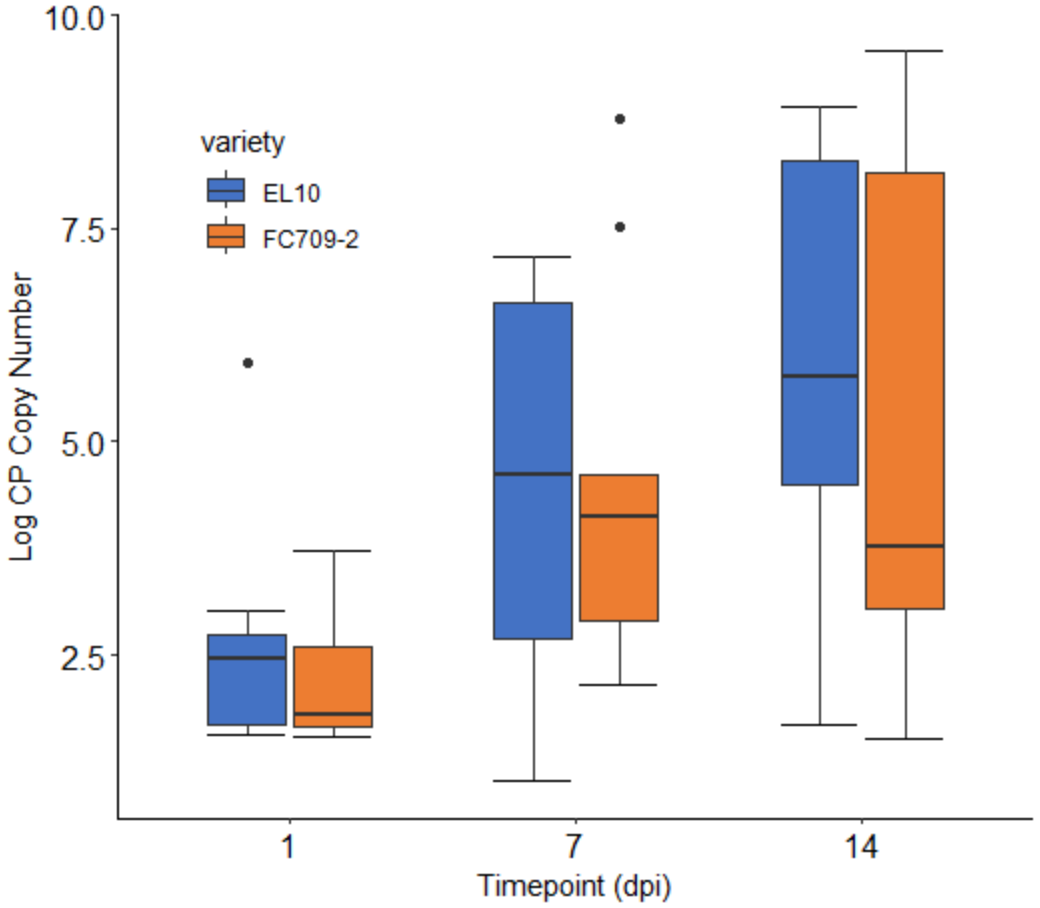

Figure 7: The average log virus copy number of BCTV infected sugar beets of two genotypes over time was determined using qPCR. The average log copy number of BCTV for n=10 replicates was determined by plotting Cq values on the generated standard curve (supplemental figure 1). Boxplot bars show the lower quartile, median, and upper quartile of the data, while round circles identify outliers. Statistical analysis was performed using a Wilcoxon test at individual time points in which no statistical significance was determined.

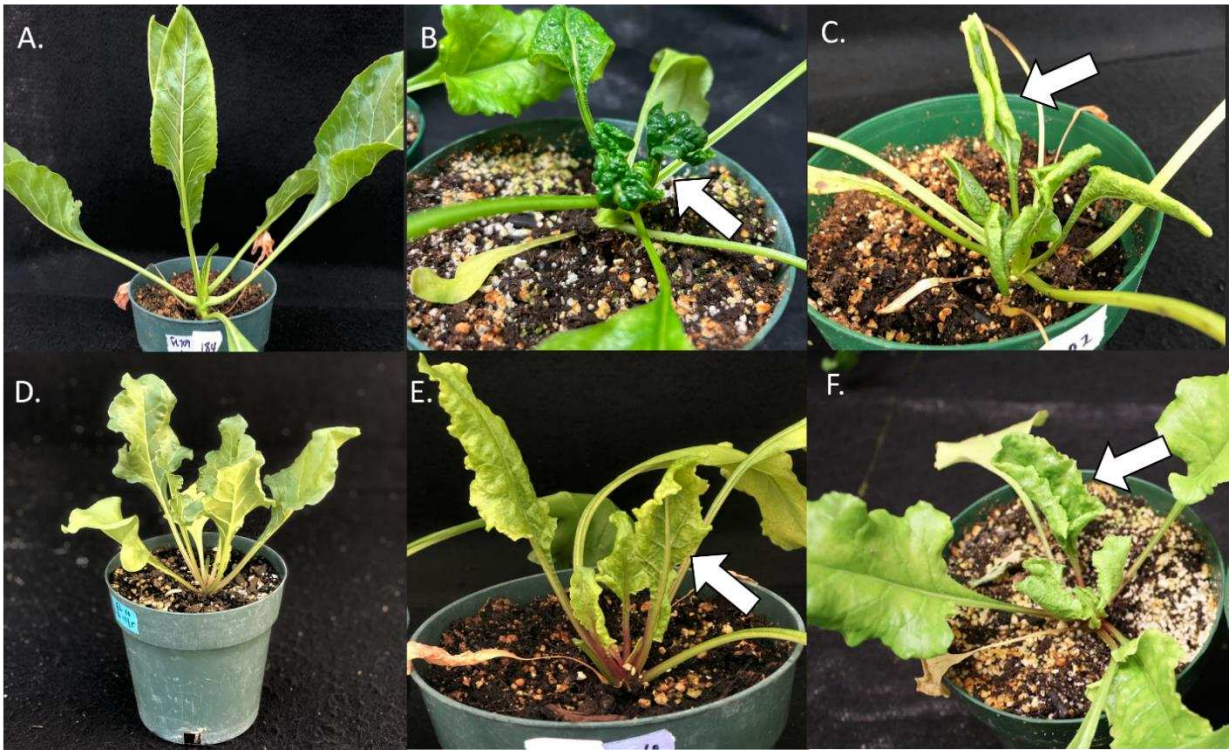

Figure 8: The range of symptoms present in the two genotypes of sugar beet at three weeks post BCTV inoculation. **(A)** Healthy FC709-2 **(B & C)** BCTV infected FC709-2 showing severe twisting and leaf curling of the new growth. **(D)** Healthy EL10 **(E & F)** BCTV infected EL10 showing vein swelling and mild leaf curling

Table 1: Summary statistics of RNA sequencing data including the number of raw reads pre and post trimming, percentage of reads with a base quality score greater than 20, as well as the number of reads mapped to the reference genome for each sample. Sample names start with biological replicate number, followed by treatment group [Uninfected (NV) or Virus-infected (V)], genotype, and timepoint collected.

Sample	Number of Raw Reads	Number of Reads Post Trimming	Total Filtered Q20 Reads (%)	Read Pairs Mapped	Percent of Reads Mapped (%)
1NV_EL_1	48,293,324	44,904,272	93	38,940,484	87
1NV_EL_7	42,762,220	39,746,024	93	34,519,504	87
1NV_EL_14	55,483,578	51,580,624	93	45,118,884	87
1V_EL_1	40,422,408	37,578,074	93	32,668,958	87
1V_EL_7	45,360,572	42,430,052	94	36,860,558	87
1V_EL_14	55,387,978	51,224,910	92	44,331,110	87
2NV_EL_1	44,874,492	41,830,228	93	36,624,298	88
2NV_EL_7	47,022,990	43,517,772	93	37,931,894	87
2NV_EL_14	40,287,002	37,598,912	93	32,942,056	88
2V_EL_1	43,003,876	40,113,082	93	34,992,884	87
2V_EL_7	42,552,140	39,528,998	93	34,355,704	87
2V_EL_14	49,262,112	45,974,844	93	39,883,712	87
3NV_EL_1	51,065,650	47,427,932	93	41,255,578	87
3NV_EL_7	57,148,808	52,898,258	93	46,830,700	89
3NV_EL_14	50,168,292	46,331,504	92	40,397,734	87
3V_EL_1	46,771,516	43,689,748	93	38,453,506	88
3V_EL_7	40,440,792	37,653,152	93	33,157,146	88
3V_EL_14	45,807,316	42,695,868	93	37,623,942	88
1NV_FC_1	45,031,540	41,939,846	93	35,292,544	84
1NV_FC_7	50,131,972	46,799,002	93	39,333,252	84
1NV_FC_14	41,058,942	38,491,994	94	32,583,362	85
1V_FC_1	42,086,042	39,442,548	94	33,903,052	86
1V_FC_7	42,263,018	39,276,510	93	33,231,848	85
1V_FC_14	40,168,138	37,558,980	94	31,304,694	83
2NV_FC_1	55,147,532	51,028,996	93	43,617,592	85
2NV_FC_7	43,273,998	40,188,746	93	34,037,012	85
2NV_FC_14	55,419,432	51,547,458	93	43,757,716	85
2V_FC_1	52,830,768	48,793,150	92	41,759,822	86
2V_FC_7	40,741,676	37,797,316	93	31,977,238	85
2V_FC_14	43,734,340	40,769,648	93	34,388,010	84
3NV_FC_1	52,137,982	46,102,870	88	38,833,006	84
3NV_FC_7	40,740,442	36,332,888	89	30,697,182	84
3NV_FC_14	56,082,754	51,535,190	92	44,684,036	87
3V_FC_1	45,139,722	40,553,834	90	35,066,036	86
3V_FC_7	35,126,710	32,046,746	91	27,908,410	87
3V_FC_14	94,077,834	83,011,782	88	71,390,024	86
Mean	47,814,109	44,165,049	92	38,073,708	86

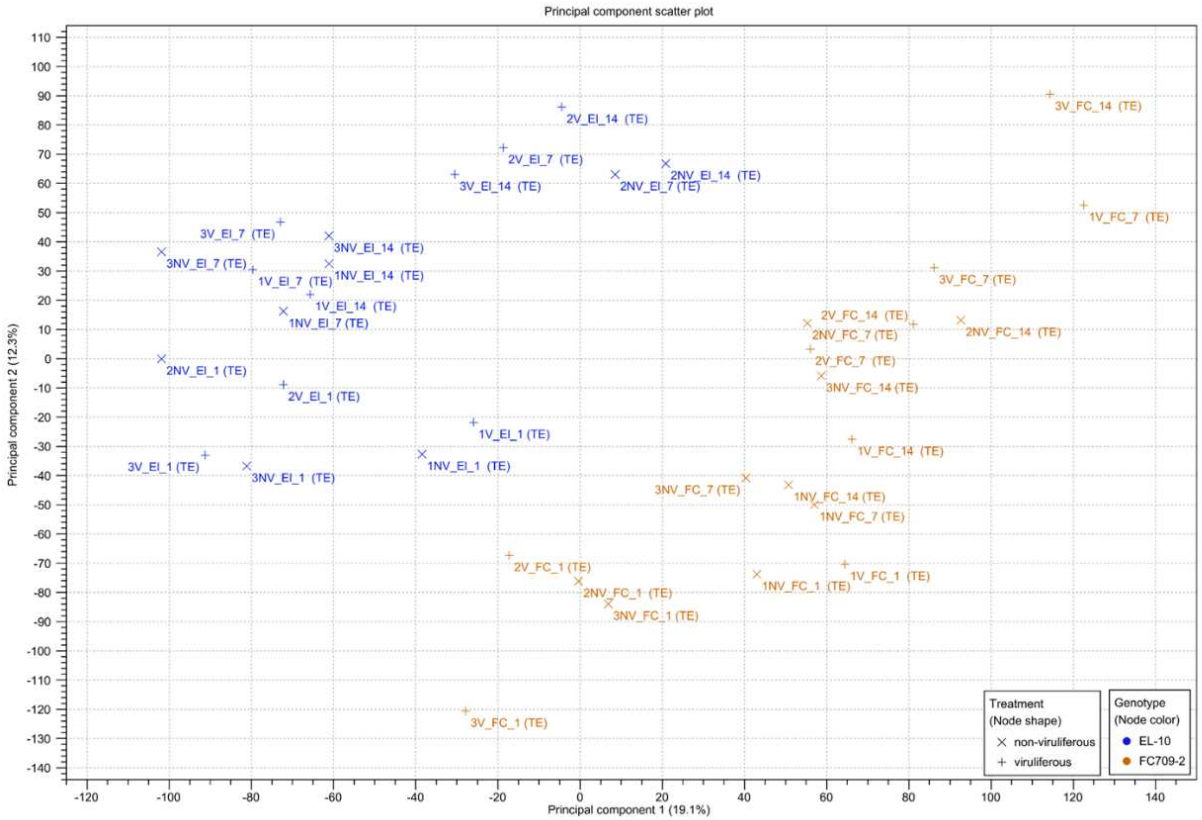

Figure 9: Principal component analysis (PCA) plot showing the transcriptomic profiles of two sugar beet genotypes in response to treatment at three timepoints.

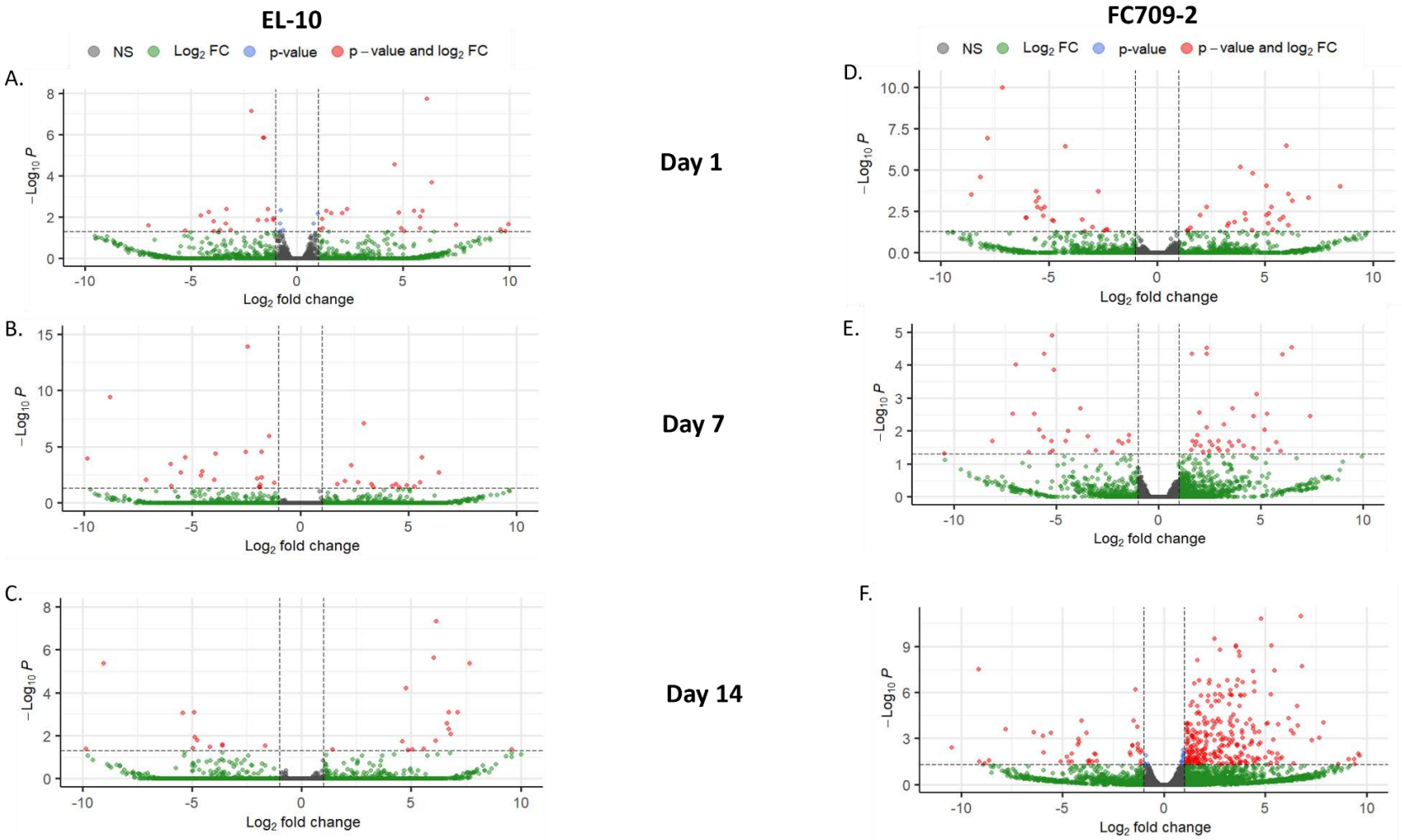

Figure 10: Volcano plots showing the number of differentially expressed transcripts for each comparison at day 1, day 7 and day 14. Grey points represent transcripts of no significance, green points indicate transcripts with expression levels above a log2 fold change of |1|, blue points indicate a significant FDR *p*-value < 0.05, and red points show transcripts with a significant log fold change and FDR *p*-value.

Table 2: List of top 30 (15 upregulated and 15 downregulated) differentially expressed transcripts (DETs) found in **day 1 EL10** comparison of mock-inoculated vs BCTV-inoculated plants.

Transcript ID	Log2 Fold Change	Adj. P value	Gene Description
Bevul.9G042800.5	9.95	0.022	E3 ubiquitin-protein ligase PRT6 isoform X1
Bevul.7G049000.2	9.81	4.79E-02	serine/threonine protein phosphatase 2A 57 kDa regulatory subunit B' theta isoform-like
Bevul.7G076300.1	9.58	3.91E-02	mediator of RNA polymerase II transcription subunit 33A-like isoform X2
Bevul.2G008000.3	7.47	2.21E-02	Sirohydrochlorin ferrochelatase, chloroplastic
Bevul.9G069100.1	6.32	1.97E-04	1D-myo-inositol 2-amino-2-deoxy-alpha-D-glucopyranoside ligase
Bevul.7G030800.12	6.10	1.80E-08	general transcription factor 3C polypeptide 2
Bevul.9G002100.2	5.91	0.005	helicase-like transcription factor CHR28 isoform X1
Bevul.9G069300.3	5.79	3.32E-02	protein STRUBBELIG-RECEPTOR FAMILY 3-like isoform X1
Bevul.2G179600.2	5.78	0.009	phospholipase D alpha 1
Bevul.2G200000.2	5.51	4.90E-03	E3 ubiquitin-protein ligase At3g02290-like isoform X1
Bevul.2G036800.15	5.04	0.047	probable choline kinase 2
Bevul.2G022400.5	4.91	0.033	tuftelin-interacting protein 11
Bevul.2G055700.4	4.80	0.006	inositol hexakisphosphate and diphosphoinositol-pentakisphosphate kinase 2 isoform X2
Bevul.2G218200.4	4.60	2.64E-05	histone acetyltransferase HAC1 isoform X1
Bevul.9G144500.2	2.34	0.004	receptor protein kinase TMK1-like
Bevul.3G041000.1	-1.56	1.36E-06	bark storage protein A-like
Bevul.2G157200.1	-1.61	1.36E-06	probable phosphoribosylformylglycinamidine synthase, chloroplastic/mitochondrial
Bevul.1G104500.1	-1.83	0.013	protein EXORDIUM-like
Bevul.2G177000.2	-2.15	7.04E-08	protein transport protein Sec24-like At3g07100
Bevul.1G116800.1	-3.14	0.040	caffeic acid 3-O-methyltransferase-like
Bevul.9G203700.2	-3.33	0.004	uncharacterized protein LOC111019049
Bevul.7G013100.3	-3.37	1.98E-02	protein SCAR2 isoform X1
Bevul.9G214200.2	-3.66	0.040	homeobox-leucine zipper protein ATHB-15 isoform X1
Bevul.2G094800.4	-3.93	0.047	phospholipid-transporting ATPase 2-like isoform X1
Bevul.2G179600.3	-3.95	0.015	phospholipase D alpha 1
Bevul.9G061300.3	-4.18	5.63E-03	protein ROLLING AND ERECT LEAF 2
Bevul.2G177900.3	-4.55	8.32E-03	Protein kinase superfamily protein
Bevul.9G144400.4	-5.30	4.27E-02	protein LNK1-like isoform X1
Bevul.2G055900.3	-7.01	2.44E-02	CSC1-like protein RXW8 isoform X1
Bevul.7G052600.17	-8.28	8.05E-09	conserved oligomeric Golgi complex subunit 4

Table 3: List of top 30 (15 upregulated and 15 downregulated) differentially expressed transcripts (DETs) found in **day 7 EL10** comparison of mock-inoculated vs BCTV-inoculated plants.

Transcript ID	Log2 Fold Change	Adj. P value	Gene Description
Bevul.2G101700.1	10.26	0.038	elongator complex protein 1-like isoform X2
Bevul.2G036800.15	10.09	0.030	probable choline kinase 2
Bevul.2G014900.3	6.40	0.002	protein DDB_G0276689 isoform X4
Bevul.2G042100.1	5.61	7.89E-05	tetratricopeptide-like helical domain, Protein SirB1
Bevul.8G045000.1	5.51	0.013	hypothetical protein SOVF_133670
Bevul.7G036800.1	5.26	0.034	photoconvertible water-soluble chlorophyll-biniding protein
Bevul.2G001400.1	4.91	0.027	DNA topoisomerase 2-binding protein 1
Bevul.9G109900.2	4.55	0.038	geranylgeranyl transferase type-2 subunit beta 1-like
Bevul.9G010200.3	4.40	0.019	L-aspartate oxidase, chloroplastic-like
Bevul.9G004200.7	4.23	0.030	Tubulin polyglutamylase complex subunit 1
Bevul.2G011000.2	3.37	0.038	probable protein phosphatase 2C 60 isoform X2
Bevul.4G242100.1	3.28	0.019	linoleate 13S-lipoxygenase 2-1, chloroplastic
Bevul.7G049100.3	2.93	7.68E-08	putative transcription elongation factor SPT5 homolog 1
Bevul.4G242300.1	2.68	0.013	linoleate 13S-lipoxygenase 2-1, chloroplastic-like
Bevul.2G108900.2	2.35	4.26E-04	SAC3 family protein A-like isoform X1
Bevul.4G236400.1	-2.46	1.21E-14	anion permease
Bevul.4G237300.1	-2.53	2.60E-05	polyadenylate-binding protein RBP47B
Bevul.2G029200.2	-3.93	4.12E-05	E3 ubiquitin-protein ligase SHPRH isoform X1
Bevul.9G197700.7	-3.99	0.008	probable leucine-rich repeat receptor-like serine/threonine-protein kinase
Bevul.2G022800.5	-4.54	0.001	protein tesmin/TSO1-like CXC 4
Bevul.2G194900.2	-4.61	0.003	pheophytinase, chloroplastic isoform X1
Bevul.4G237700.1	-4.63	3.02E-36	---NA---
Bevul.2G090500.1	-5.34	7.89E-05	E3 ubiquitin-protein ligase WAV3-like isoform X2
Bevul.7G052800.5	-5.53	0.002	TSL-kinase interacting protein 1
Bevul.7G076300.4	-5.98	0.029	mediator of RNA polymerase II transcription subunit 33A-like isoform X2
Bevul.2G216400.3	-6.01	3.29E-04	Zinc-finger domain of monoamine-oxidase A repressor R1 protein
Bevul.2G205300.2	-7.13	0.008	regulator of nonsense transcripts 2 isoform X1
Bevul.2G042100.2	-8.81	3.53E-10	tetratricopeptide-like helical domain, Protein SirB1
Bevul.7G013100.3	-9.86	1.01E-04	protein SCAR2 isoform X1
Bevul.4G236900.1	-10.32	0.024	putative RNA-binding protein pno1

Table 4: List of top 30 (15 upregulated and 15 downregulated) differentially expressed transcripts (DETs) found in **day 14 EL10** comparison of mock-inoculated vs BCTV-inoculated plants.

Transcript ID	Log2 Fold Change	Adj. P value	Gene Description
Bevul.9G181800.6	9.59	0.043	serine/threonine-protein kinase SRK2I-like isoform 1
Bevul.2G014900.3	7.67	4.21E-06	protein DDB_G0276689 isoform X4
Bevul.2G027300.5	7.10	0.001	uncharacterized protein LOC104594488 isoform X2
Bevul.2G225800.3	6.79	0.008	serine/threonine-protein phosphatase PP1 isozyme 4
Bevul.7G066200.3	6.70	0.005	Guanine nucleotide exchange factor SPIKE 1
Bevul.2G039700.2	6.70	0.001	E3 ubiquitin-protein ligase KEG
Bevul.2G200000.2	6.62	0.003	E3 ubiquitin-protein ligase At3g02290-like isoform X1
Bevul.7G037100.1	6.12	4.72E-08	photoconvertible water-soluble chlorophyll-biniding protein
Bevul.9G139200.1	6.11	0.017	MADS-box protein JOINTLESS-like isoform X1
Bevul.7G036800.1	6.02	2.26E-06	photoconvertible water-soluble chlorophyll-biniding protein
Bevul.2G105200.2	5.58	0.040	tyrosine-phosphatase
Bevul.2G230800.1	5.06	0.042	scarecrow-like protein 14
Bevul.9G144400.2	4.84	0.047	protein LNK1-like isoform X1
Bevul.2G112800.5	4.77	6.18E-05	ethylene-responsive transcription factor RAP2-7 isoform X2
Bevul.7G052600.17	4.60	0.018	conserved oligomeric Golgi complex subunit 4
Bevul.5G184200.1	1.40	0.044	basic endochitinase
Bevul.9G107100.1	-1.67	0.028	Phosphatase PHOSPHO-type
Bevul.6G063700.1	-3.62	0.028	putative S-phase kinase-associated protein
Bevul.2G218200.4	-3.62	0.026	histone acetyltransferase HAC1 isoform X1
Bevul.9G059500.6	-4.18	0.033	CCR4-NOT transcription complex subunit 4
Bevul.7G103100.4	-4.78	0.016	(p)ppGpp synthetase/guanosine-3',5'-bis(diphosphate) 3'-pyrophosphohydrolase
Bevul.9G214700.5	-4.89	0.011	ATP-dependent zinc metalloprotease FtsH
Bevul.7G054500.9	-4.92	0.001	helicase protein MOM1-like isoform X1
Bevul.2G031400.4	-4.96	0.038	autophagy-related protein 18c-like
Bevul.2G197300.2	-5.43	0.001	zinc finger CCCH domain-containing protein 27 isoform X1
Bevul.9G055200.3	-8.52	1.94E-09	tRNA ligase 1 isoform X1
Bevul.2G112800.4	-9.04	4.21E-06	ethylene-responsive transcription factor RAP2-7 isoform X2
Bevul.2G234200.4	-9.85	0.041	uncharacterized protein LOC110785510 isoform X1
Bevul.2G205300.2	-10.81	0.017	regulator of nonsense transcripts 2 isoform X1
Bevul.7G061400.5	-10.97	0.008	Hyccin

Table 5: List of top 30 (15 upregulated and 15 downregulated) differentially expressed transcripts (DETs) found in **day 1 FC709-2** comparison of mock-inoculated vs BCTV-inoculated plants.

Transcript ID	Log2 Fold Change	Adj. P value	Gene Description
Bevul.2G022400.6	10.61	0.023	tuftelin-interacting protein 11
Bevul.9G196100.1	10.18	1.80E-02	polyadenylate-binding protein-interacting protein 4-like
Bevul.7G073700.7	8.47	9.22E-05	Dynamin GTPase protein
Bevul.4G049100.1	7.00	4.57E-04	(-)-germacrene D synthase
Bevul.2G014000.1	6.24	0.001	type I ribosome-inactivating protein trichoanguina-like
Bevul.7G032200.5	6.08	2.60E-04	pleiotropic drug resistance protein 2 isoform X1
Bevul.2G105200.6	6.05	0.022	tyrosine-phosphatase
Bevul.7G007800.1	5.97	3.13E-07	replication protein A 70 kDa DNA-binding subunit A-like isoform X1
Bevul.2G200200.3	5.83	0.007	UVB photoreceptor UVR8 from Arabidopsis thaliana and UV-induced structural changes at 120K
Bevul.9G046100.3	5.68	9.43E-03	lysM domain receptor-like kinase 3
Bevul.7G031900.6	5.36	0.040	BTB/POZ domain-containing protein FBL11 isoform X4
Bevul.2G101600.19	5.28	0.002	Golgi to ER traffic 4
Bevul.9G197600.1	5.16	0.004	LEA5
Bevul.9G207800.4	5.15	1.56E-02	magnesium transporter MRS2-4-like
Bevul.4G034400.1	5.06	0.005	probable disease resistance protein At4g27220
Bevul.9G072900.7	-4.86	0.011	probable methyltransferase PMT3 isoform X1
Bevul.4G085400.1	-5.21	0.002	trans-resveratrol di-O-methyltransferase-like
Bevul.7G001900.4	-5.27	0.006	probable inactive receptor kinase At4g23740
Bevul.7G093600.4	-5.35	0.002	ABC transporter C family member 14-like
Bevul.7G042700.4	-5.48	0.000	E3 ubiquitin-protein ligase UPL7 isoform X1
Bevul.9G137200.8	-5.55	0.002	E3 ubiquitin-protein ligase UPL3-like
Bevul.7G001900.3	-5.60	1.83E-04	probable inactive receptor kinase At4g23740
Bevul.2G065400.6	-5.60	0.001	uncharacterized protein LOC109849903
Bevul.2G234200.4	-6.06	0.007	uncharacterized protein LOC110785510 isoform X1
Bevul.9G077800.2	-6.07	0.007	transmembrane E3 ubiquitin-protein ligase FLY1-like isoform X2
Bevul.7G002600.2	-7.15	9.60E-11	serine/threonine-protein kinase STN8, chloroplastic
Bevul.2G072100.3	-7.84	1.11E-07	alpha-1,4 glucan phosphorylase L isozyme, chloroplastic/amyloplastic isoform X2
Bevul.2G022400.2	-8.17	2.45E-05	tuftelin-interacting protein 11
Bevul.9G171300.2	-8.60	3.03E-04	C-terminal binding protein AN
Bevul.9G018700.3	-11.10	1.56E-11	UDP-glucose 6-dehydrogenase 1

Table 6: List of top 30 (15 upregulated and 15 downregulated) differentially expressed transcripts (DETs) found in **day 7 FC709-2** comparison of mock-inoculated vs BCTV-inoculated plants.

Transcript ID	Log2 Fold Change	Adj. P value	Gene Description
Bevul.2G038700.1	10.42	0.020	protein unc-13 homolog
Bevul.2G200000.2	7.41	3.41E-03	E3 ubiquitin-protein ligase At3g02290-like isoform X1
Bevul.2G029200.1	6.50	2.82E-05	E3 ubiquitin-protein ligase SHPRH isoform X1
Bevul.9G065100.1	6.06	4.67E-05	BTB/POZ domain-containing protein At3g22104 isoform X2
Bevul.7G081000.1	5.97	0.040	putative transcription factor Hap3/NF-YB family
Bevul.9G147400.2	5.76	0.022	chaperone protein dnaJ A6, chloroplastic
Bevul.9G104500.1	5.36	0.037	O-acyltransferase WSD1
Bevul.9G167200.1	5.30	2.94E-03	chaperone protein dnaJ 10-like isoform X1
Bevul.9G167200.6	5.18	0.009	chaperone protein dnaJ 10-like isoform X1
Bevul.5G011000.1	4.80	7.60E-04	primary amine oxidase 2 isoform X1
Bevul.2G087200.1	4.66	0.033	TELO2 interacting protein 1
Bevul.2G088500.2	4.64	0.003	probable potassium transporter 13 isoform X2
Bevul.2G112800.4	4.16	0.027	ethylene-responsive transcription factor RAP2-7 isoform X2
Bevul.2G036800.8	3.91	2.02E-02	probable choline kinase 2
Bevul.8G066800.1	3.63	0.002	(3S,6E)-nerolidol synthase 1
Bevul.2G215400.2	-5.11	1.39E-04	14-3-3-like protein GF14 psi
Bevul.6G158500.1	-5.16	0.039	ubiquitin-like domain-containing CTD phosphatase 1 isoform X1
Bevul.9G065100.3	-5.22	1.24E-05	BTB/POZ domain-containing protein At3g22104 isoform X2
Bevul.2G220100.3	-5.22	0.020	CWF19-like protein 2 isoform X2
Bevul.3G028600.1	-5.29	0.043	jasmonate-induced protein homolog
Bevul.2G022500.2	-5.61	4.48E-05	putative digestive organ expansion factor
Bevul.9G041600.3	-5.64	0.015	uncharacterized protein LOC18034531 isoform X4
Bevul.1G160000.1	-5.83	0.009	germin-like protein subfamily 1 member 17
Bevul.9G059500.6	-6.09	0.003	CCR4-NOT transcription complex subunit 4
Bevul.2G072100.3	-6.35	0.043	alpha-1,4 glucan phosphorylase L isozyme, chloroplastic/amyloplastic isoform X2
Bevul.9G013800.6	-6.98	9.48E-05	disease resistance RPP13-like protein 4 isoform X1
Bevul.2G230800.5	-7.15	2.99E-03	scarecrow-like protein 14
Bevul.9G230500.4	-8.12	0.020	pentatricopeptide repeat-containing protein At1g51965, mitochondrial-like
Bevul.2G105200.7	-10.49	0.047	tyrosine-phosphatase
Bevul.9G118100.2	-11.45	0.020	ABC transporter G family member 29

Table 7: List of top 30 (15 upregulated and 15 downregulated) differentially expressed transcripts (DETs) found in **day 14 FC709-2** comparison of mock-inoculated vs BCTV-inoculated plants.

Transcript ID	Log2 Fold Change	Adj. P value	Gene Description
Bevul.2G044800.5	10.93	3.34E-06	Protein LNK2
Bevul.4G034400.1	10.28	3.53E-03	probable disease resistance protein At4g27220
Bevul.9G002100.2	9.63	0.013	helicase-like transcription factor CHR28 isoform X1
Bevul.2G022400.2	9.58	0.010	tuftelin-interacting protein 11
Bevul.9G192000.1	9.41	0.044	post-illumination chlorophyll fluorescence increase
Bevul.9G116000.2	9.39	0.023	auxin-responsive protein IAA7
Bevul.2G072800.4	9.11	0.021	sister chromatid cohesion protein SCC2 isoform X2
Bevul.7G052800.5	8.60	4.48E-02	TSL-kinase interacting protein 1
Bevul.6G197000.1	7.85	9.27E-05	ethylene-responsive transcription factor ERF113
Bevul.9G052800.1	7.80	1.67E-26	putative peroxidase
Bevul.9G194500.1	7.65	0.001	caffeic acid 3-O-methyltransferase-like
Bevul.6G015500.1	7.30	0.001	transcription factor SPT20 homolog
Bevul.9G003400.1	6.84	6.14E-13	antiviral protein PAP
Bevul.1G039600.1	6.79	1.91E-08	glucan endo-1,3-beta-glucosidase
Bevul.5G033300.1	6.76	1.01E-11	pathogenesis related protein
Bevul.9G167600.2	-4.55	0.033	bifunctional dihydrofolate reductase-thymidylate synthase-like
Bevul.2G161900.3	-4.55	0.010	protein embryonic flower 1-like isoform X1
Bevul.2G022800.1	-4.71	0.032	protein tesmin/TSO1-like CXC 4
Bevul.5G060700.1	-4.78	0.015	F-box/FBD/LRR-repeat protein At4g26340-like isoform X1
Bevul.2G087400.2	-5.11	0.032	coiled-coil domain-containing protein
Bevul.2G029200.1	-5.58	4.19E-04	E3 ubiquitin-protein ligase SHPRH isoform X1
Bevul.2G117100.3	-5.93	0.008	Nuclear receptor corepressor 1 like
Bevul.2G105200.2	-5.96	0.001	tyrosine-phosphatase
Bevul.2G042100.1	-6.44	3.86E-04	tetratricopeptide-like helical domain, Protein SirB1
Bevul.2G105200.3	-7.82	2.48E-04	tyrosine-phosphatase
Bevul.9G211100.2	-8.63	2.64E-02	protein executer 1, chloroplastic isoform X1
Bevul.9G118600.6	-8.85	4.17E-02	Casein kinase 1-like protein hd16
Bevul.7G062100.16	-9.11	0.031	interactor of constitutive active ROPs 2, chloroplastic
Bevul.2G230800.5	-9.15	2.90E-08	scarecrow-like protein 14
Bevul.2G162400.3	-10.47	0.004	aminotransferase class IV

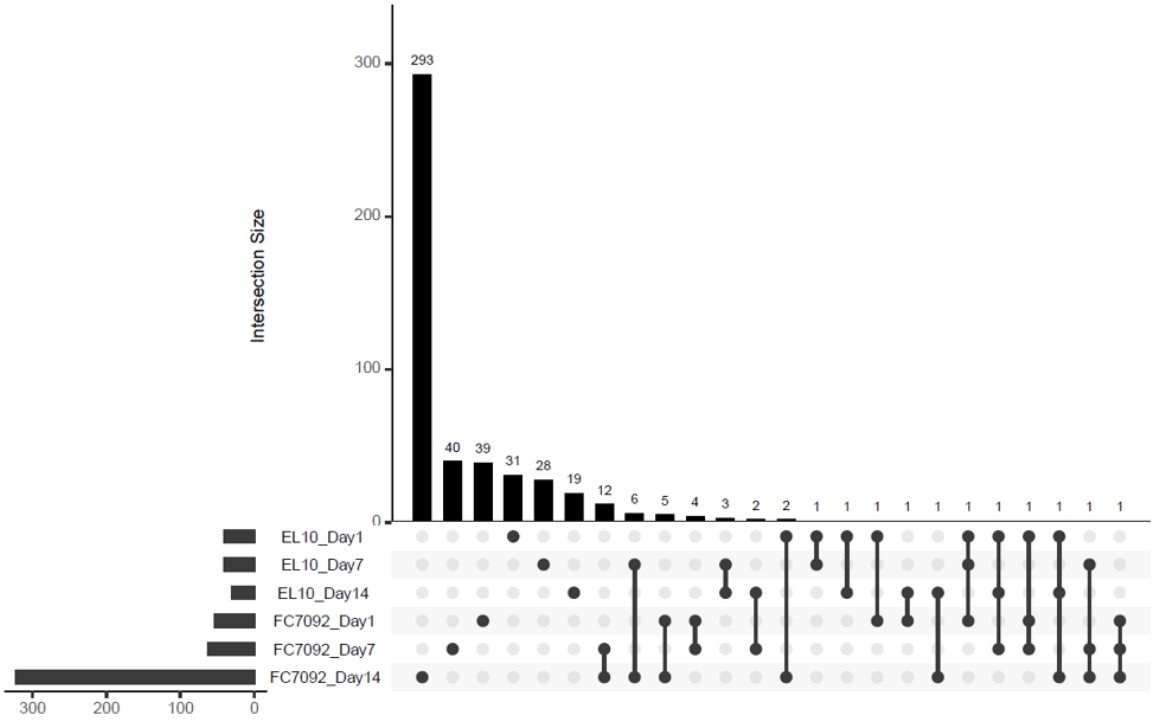

Figure 11: Upset plot showing the overlap of differentially expressed transcripts (DETs) from each genotype and timepoint. Single dots show the number of unique DETs identified, while lines connecting the dots represent the number of shared DETs between the samples.

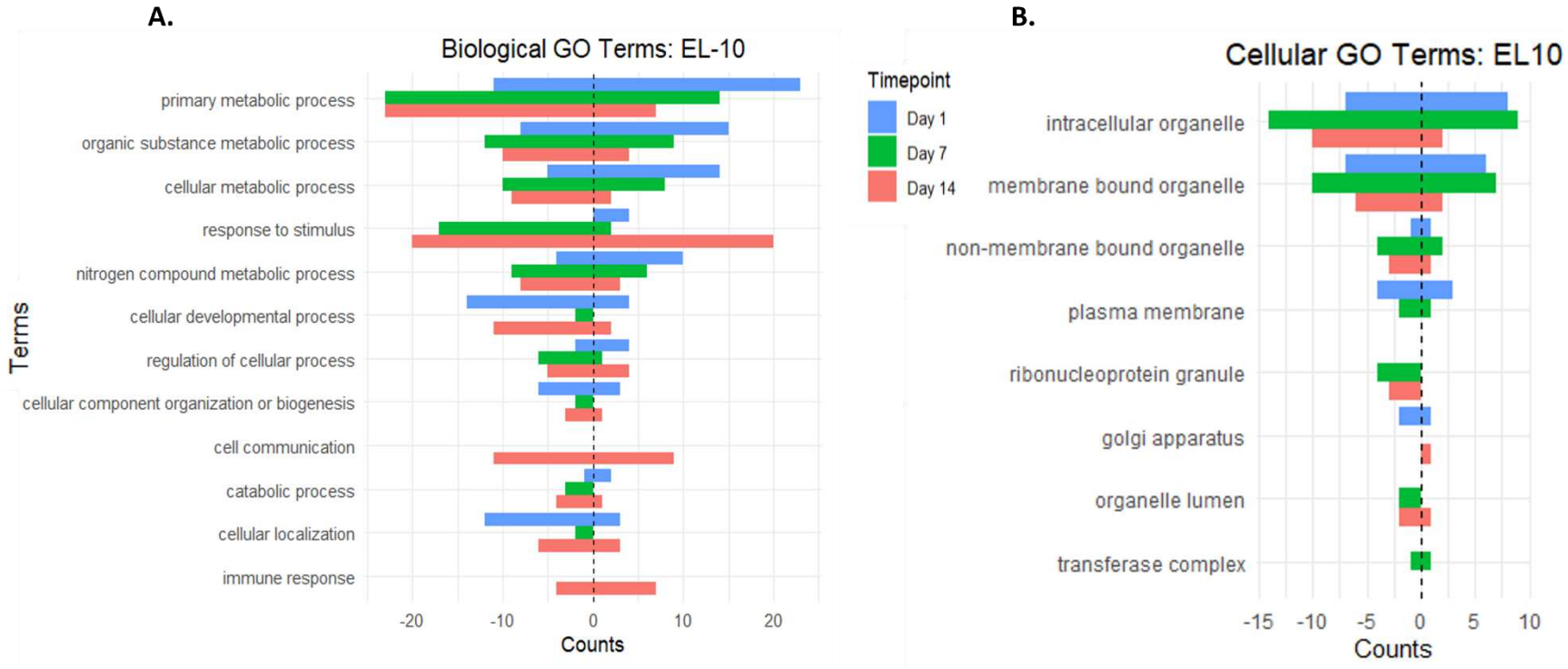

Figure 12: GO terms associated with **(A)** biological processes and **(B)** cellular components over time for the comparison of mock-inoculated to BCTV-inoculated EL10 samples. Each bar shows the number of up and down regulated counts under each parent term.

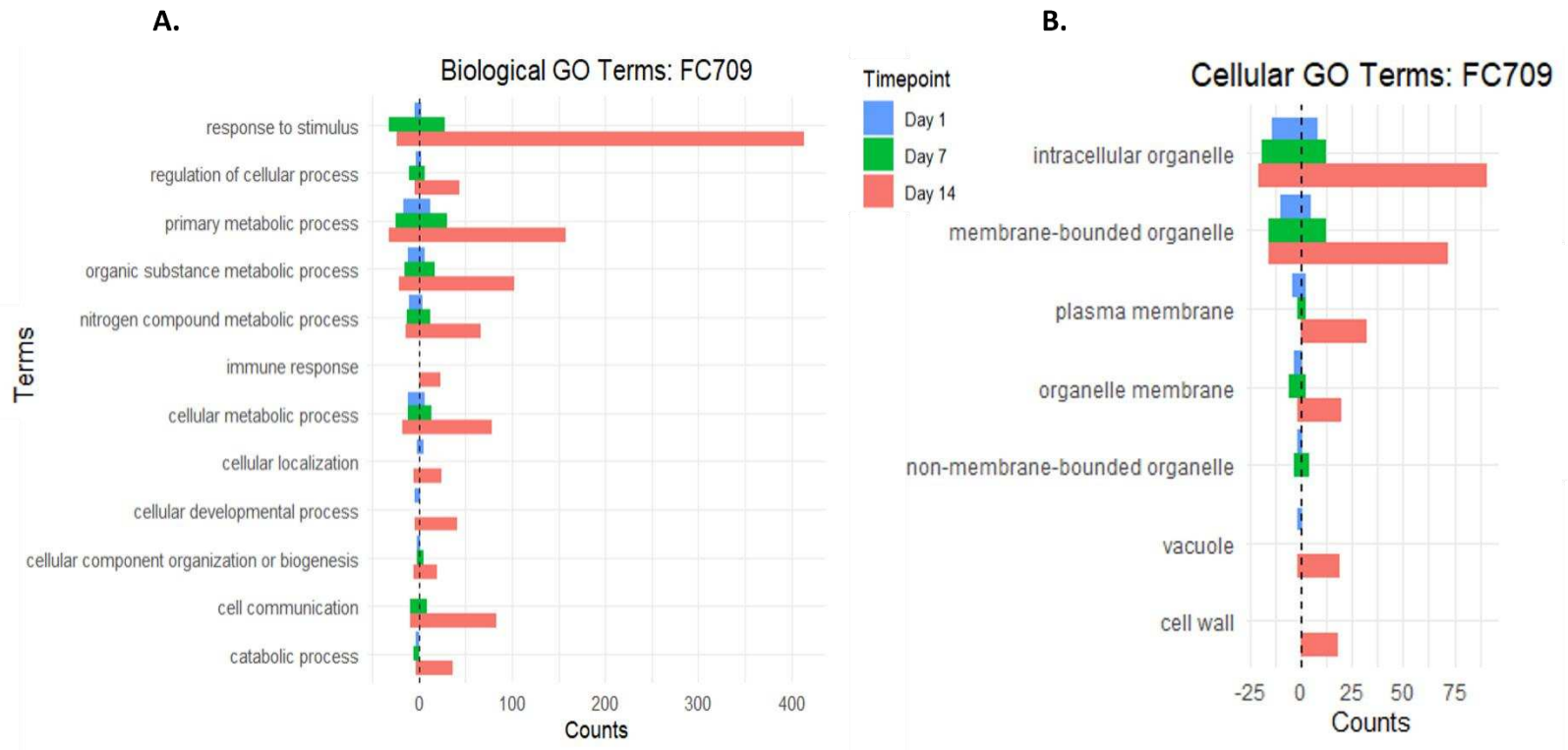

Figure 13: GO terms associated with **(A)** biological processes and **(B)** cellular components over time for the comparison of mock-inoculated to BCTV-inoculated FC709-2 samples. Each bar shows the number of up and down regulated counts under each parent term.

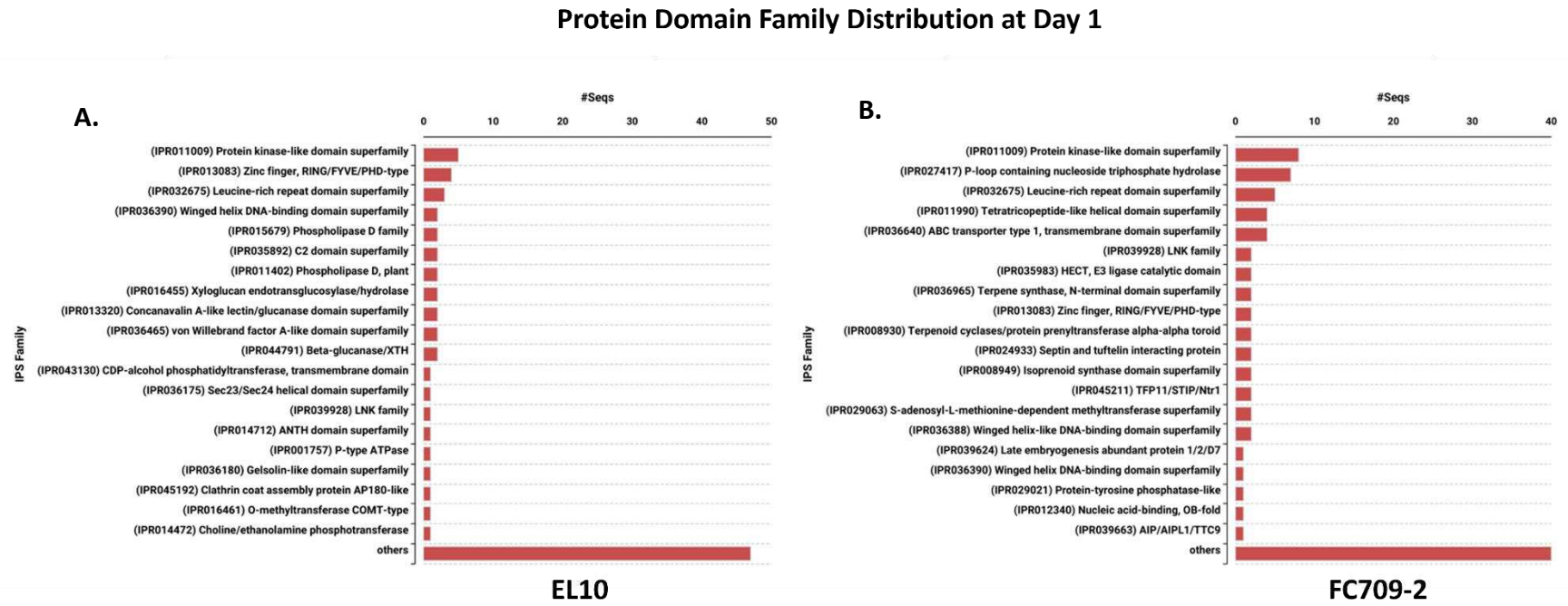

Figure 14: Protein families identified from differentially expressed transcripts found in **(A)** EL10 and **(B)** FC709-2 on day 1. Bars represent the number of terms that fall under each protein family listed on the y-axis.

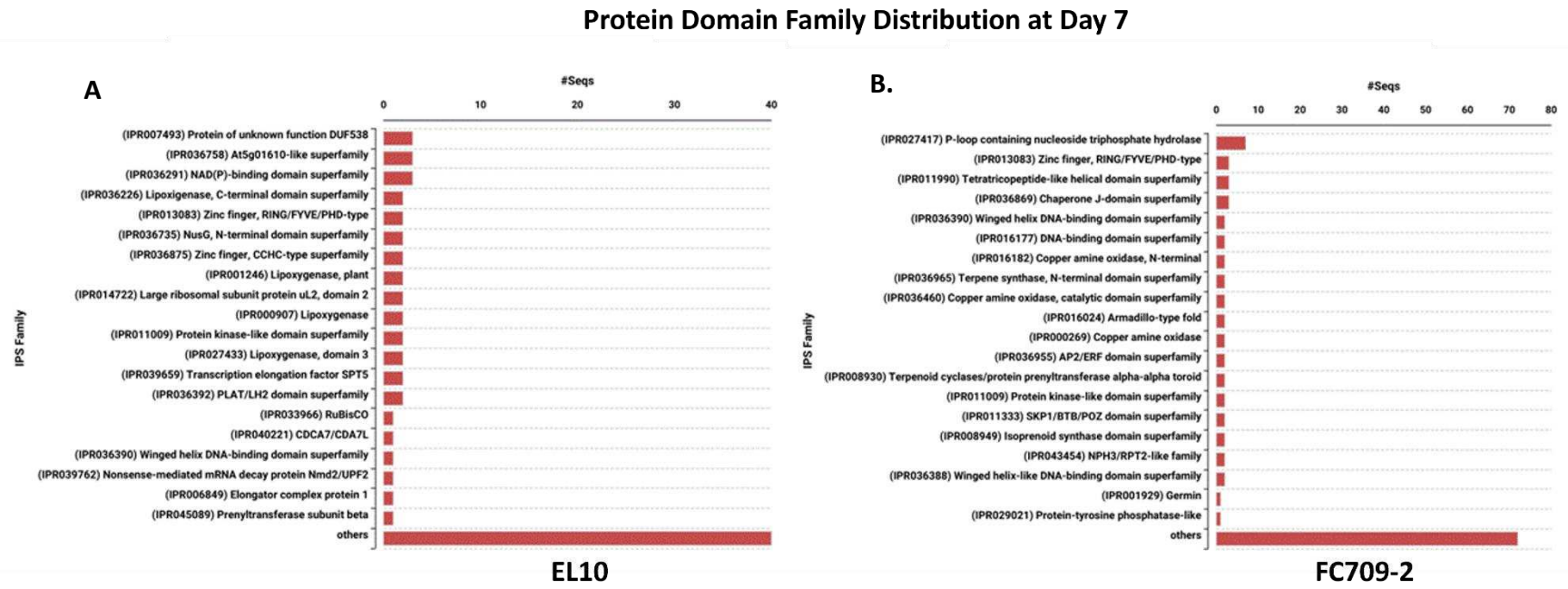

Figure 15: Protein families identified from differentially expressed transcripts found in **(A)** EL10 and **(B)** FC709-2 on day 7. Bars represent the number of terms that fall under each protein family listed on the y-axis.

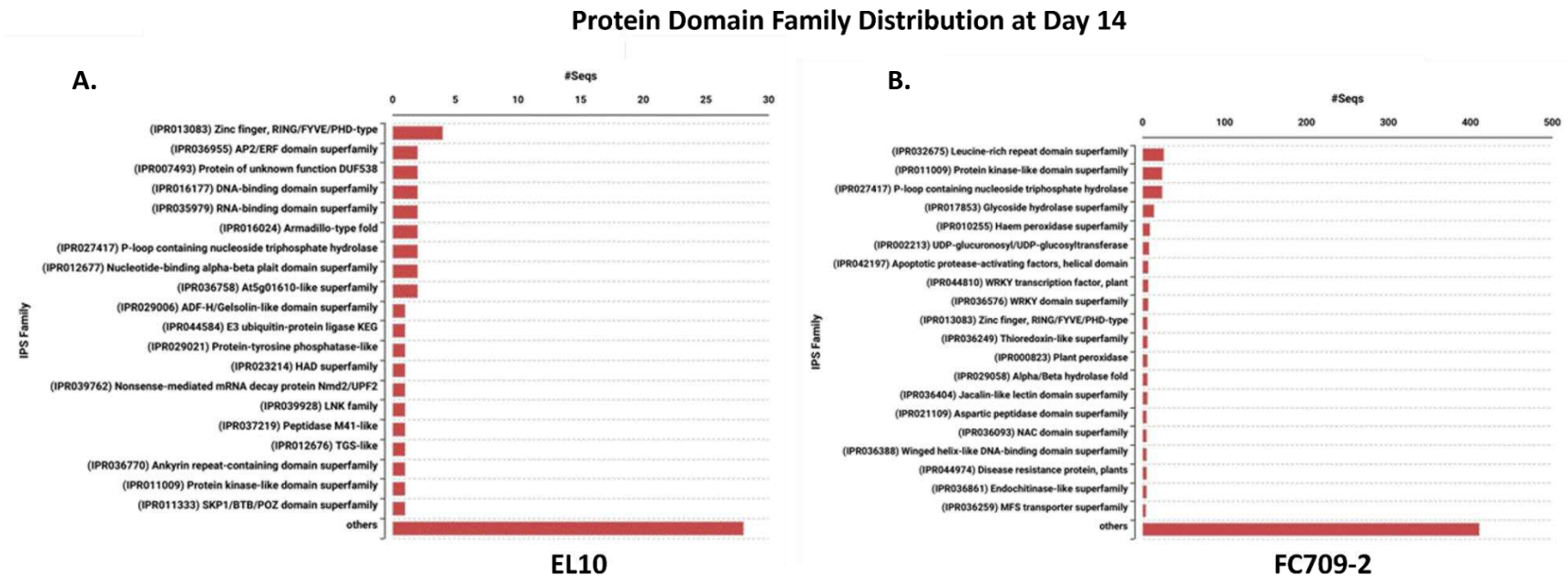

Figure 16: Protein families identified from differentially expressed transcripts found in **(A)** EL10 and **(B)** FC709-2 on day 14. Bars represent the number of terms that fall under each protein family listed on the y-axis.

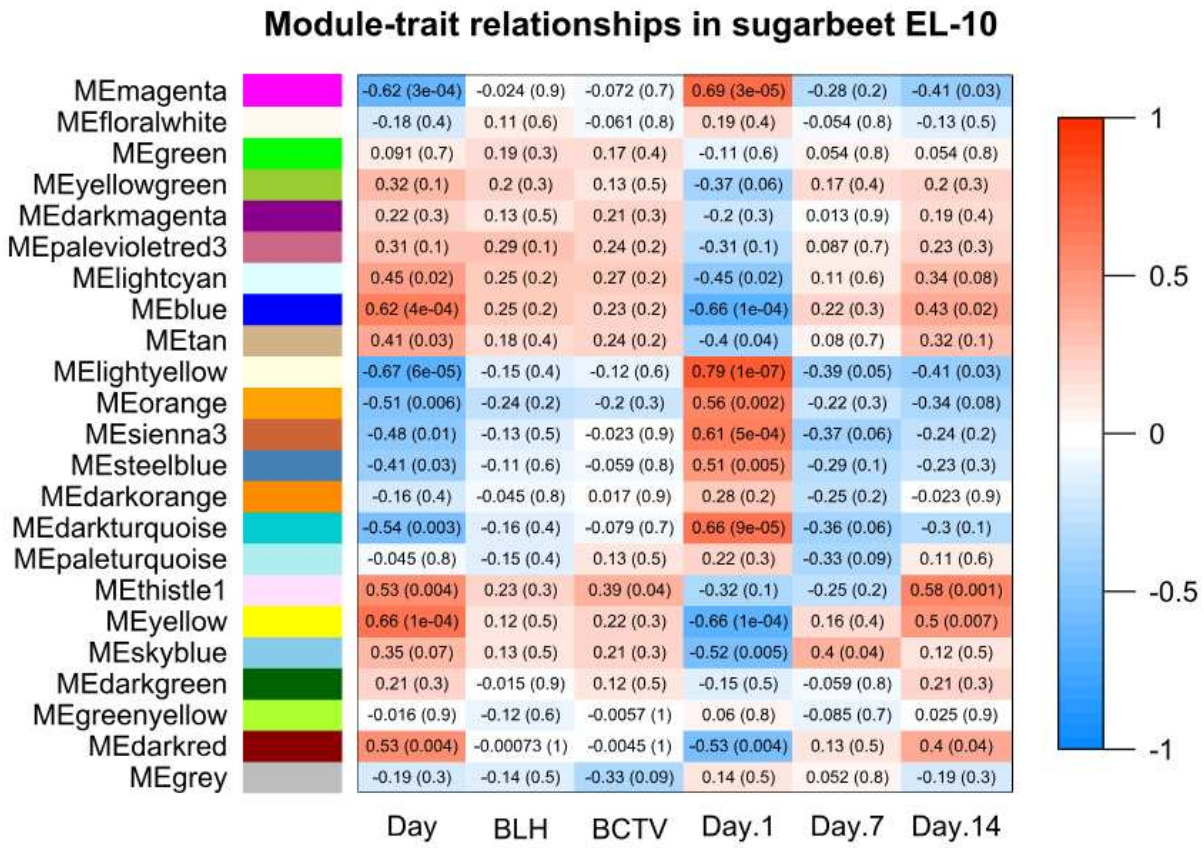

Figure 17: Module-trait relationships identified for EL10 through WGCNA. For each module identified on the y-axis, there is a corresponding correlation coefficient followed by the *p*-value in parathesis as it relates to each trait on the x-axis.

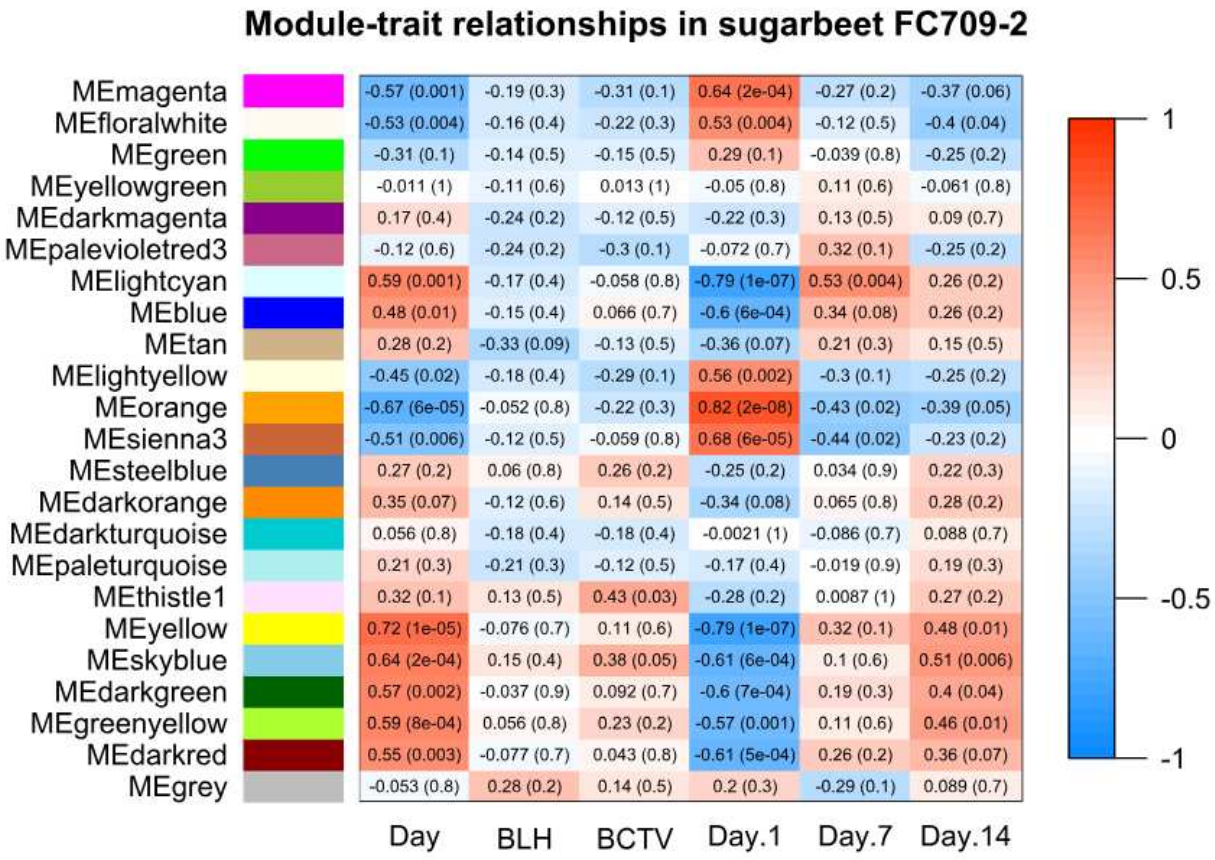

Figure 18: Module-trait relationships identified for FC709-2 through WGCNA. For each module identified on the y-axis, there is a corresponding correlation coefficient followed by the *p*-value in parathesis as it relates to each trait on the x-axis.

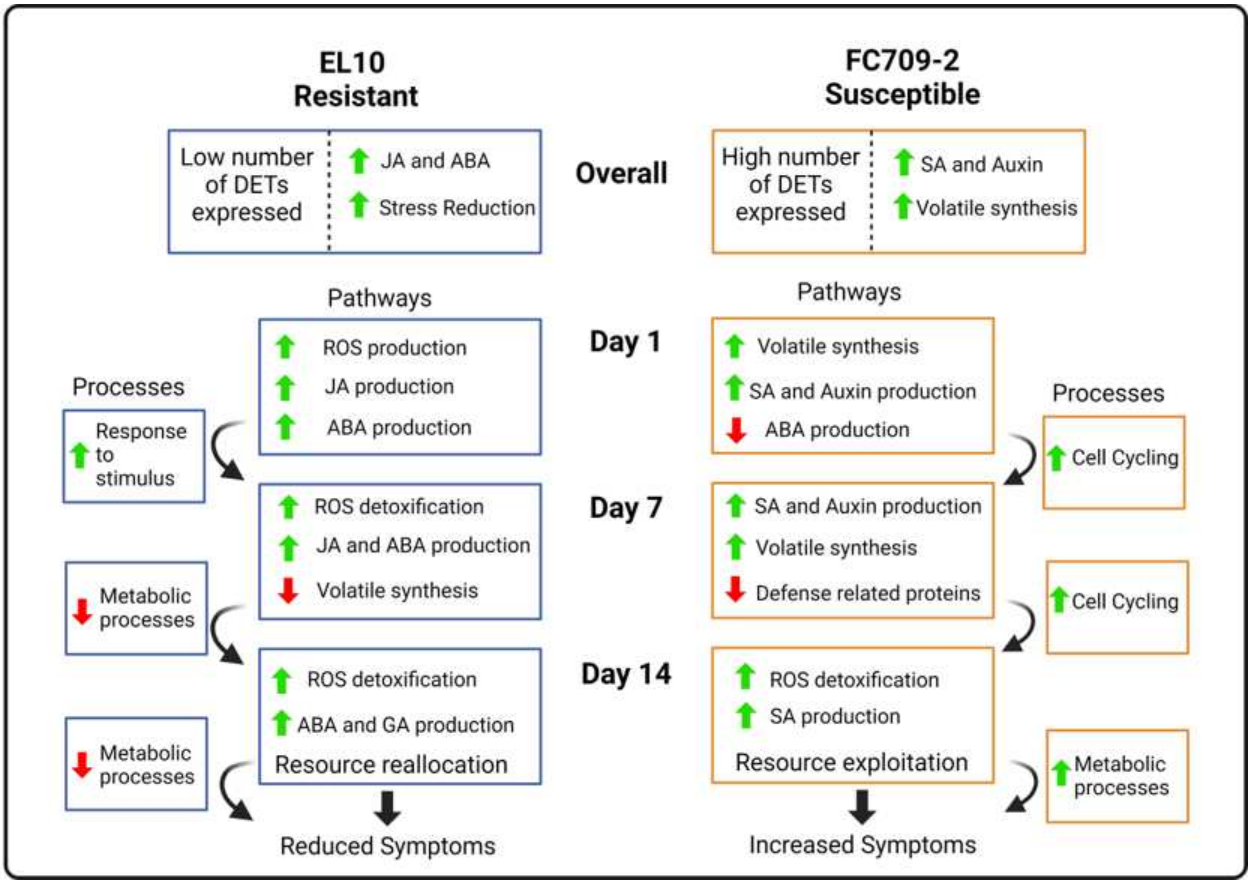

Figure 19: Summary model comparing unique pathways and processes being differentially regulated in each genotype that may contribute to reduced or increased symptoms of BCTV infection over time. This figure was created with BioRender.com and adapted from Allie et al. 2014.

REFERENCES

Abouzid, A. M., Frischmuth, T., and Jeske, H. 1988. A putative replicative form of the abutilon mosaic virus (gemini-group) in a chromatin-like structure. Mol. Gen. Genet. 212:252–258

Abraham, J., Opuni-Frimpong, E., Weissbecker, B., Schütz, S., and Angeli, S. 2014. Olfactory cues of mahogany trees to female Hypsipyla robusta. Bull. Insectology. 67:21–30

Abramovitch, R. B., Anderson, J. C., and Martin, G. B. 2006. Bacterial elicitation and evasion of plant innate immunity. Nat. Rev. Mol. Cell Biol. 7:601–611

Alazem, M., Lin, K. Y., and Lin, N. S. 2014. The abscisic acid pathway has multifaceted effects on the accumulation of bamboo mosaic virus. Mol. Plant. Microbe Interact. 27:177–189

Alazem, M., and Lin, N. 2014. Roles of plant hormones in the regulation of host–virus interactions. Mol. Plant Pathol. 16:529–540

Allie, F., Pierce, E. J., Okoniewski, M. J., and Rey, C. 2014. Transcriptional analysis of South African cassava mosaic virus-infected susceptible and tolerant landraces of cassava highlights differences in resistance, basal defense and cell wall associated genes during infection. BMC Genomics. 15:1006

Ascencio-Ibáñez, J. T., Sozzani, R., Lee, T. J., Chu, T. M., Wolfinger, R. D., Cella, R., and Hanley-Bowdoin, L. 2008. Global analysis of Arabidopsis gene expression uncovers a complex array of changes impacting pathogen response and cell cycle during geminivirus infection. Plant Physiol. 148:436–454

Ball, E. D. 1917. The beet leafhopper and the curly-leaf disease that it transmits. UAES Bull. 155:1–57

Bari, R., and Jones, J. D. G. 2009. Role of plant hormones in plant defense responses. Plant Mol. Biol. 69:473–488

Bennett, C. W. 1962. Acquisition and transmission of curly top virus by artificially fed beet leafhoppers. J. Am. Soc. Sugar Beet Technol. 11:637–648

Bennett, C. W. 1971. The curly top disease of sugar beet and other plants. Am. Phytopathol. Soc. Monogram No.7

Bhattacharya, A. N., and Lubbadah, W. F. 1971. Feeding high levels of beet pulp in high concentrate dairy rations. J. Dairy Sci. 54:95–99

Bigeard, J., Colcombet, J., and Hirt, H. 2015. Signaling mechanisms in pattern-triggered immunity (PTI). Mol. Plant. 8:521–539

Bosland, P. W., and Strausbaugh, C. A. 2010. 'NuMex Las Cruces' Cayenne Pepper. HortScience. 45:1751–1752

Carsner, E. 1933. Curly top resistance in sugar beets and tests of the resistant variety U.S. no.1. Tech. Bull. 360

Chen, L., and Gilbertson, R. L. 2016. Chapter 17: Transmission of Curtoviruses (Beet curly top virus) by the beet leafhopper (Circulifer tenellus). Pages 243–262 in: Vector-Mediated Transmission of Plant Pathogens, The American Phytopathological Society of America.

Chen, T., Lv, Y., Zhao, T., Li, N., Yang, Y., Yu, W., He, X., Liu, T., and Zhang, B. 2013. Comparative transcriptome profiling of a resistant vs. susceptible tomato (Solanum lycopersicum) cultivar in response to infection by tomato yellow leaf curl virus. PLOS ONE. 8:e80816

Clarke, S. F., Guy, P. L., Burritt, D. J., and Jameson, P. E. 2002. Changes in the activities of antioxidant enzymes in response to virus infection and hormone treatment. Physiol. Plant. 114:157–164
Cook, S. M., Khan, Z. R., and Pickett, J. A. 2007. The use of push-pull strategies in integrated pest management. Annu. Rev. Entomol. 52:375–400
Coons, G. H., Owen, F. V., and Stewart, D. 1955. Improvement of the sugar beet in the United States. Pages 89–139 in: Advances in Agronomy, A.G. Norman, ed. Academic Press.
Cooper, J. I. 1983. Responses of plants to viruses: proposals for the use of terms. Phytopathology. 73:127
Cowles, K. N., Groves, R. L., and Barak, J. D. 2018. Leafhopper-induced activation of the jasmonic acid response benefits salmonella enterica in a flagellum-dependent manner. Front. Microbiol. 9
Creamer, R. 2020. Chapter 37 - Beet curly top virus transmission, epidemiology, and management. Pages 521–527 in: Applied Plant Virology, Applied Plant Virology. Academic Press.
Dáder, B., Legarrea, S., Moreno, A., Plaza, M., Carmo-Sousa, M., Amor, F., Viñuela, E., and Fereres, A. 2015. Control of insect vectors and plant viruses in protected crops by novel pyrethroid-treated nets. Pest Manag. Sci. 71:1397–1406
Dorn, K., Fenwick, A., and Strausbaugh, C. 2021. Beet curly top resistance in USDA-ARS plant introduction lines of sugar beet, 2020. Plant Dis. Manag. Rep. 15:2
Douglass, J. R., and Cook, W. C. 1952. The beet leafhopper. in: Insects: the yearbook of agriculture, U.S. Department of Agriculture.
Esau, K. 1976. Hyperplastic phloem and its plastids in spinach infected with the curly top virus. Ann. Bot. 40:637–644
Esau, K., and Hoefert, L. L. 1973. Particles and associated inclusions in sugar beet infected with the curly top virus. Virology. 56:454–464
Eujayl, I., Strausbaugh, C., and Lu, C. 2016. Registration of sugar beet doubled haploid line KDH13 with resistance to beet curly top. J. Plant Regist. 10:93–96
Fernando Gil, J., Wibberg, D., Eini, O., Savenkov, E. I., Varrelmann, M., and Liebe, S. 2020. Comparative transcriptome analysis provides molecular insights into the interaction of beet necrotic yellow vein virus and beet soil-borne mosaic virus with their host sugar beet. Viruses. 12:76
Fraser, R. S. S., and Whenham, R. J. 1989. Abscisic acid metabolism in tomato plants infected with tobacco mosaic virus: relationships with growth, symptoms and the Tm-1 gene for TMV resistance. Physiol. Mol. Plant Pathol. 34:215–226
Gholizadeh, A. 2016. DUF538 protein superfamily is predicted to be chlorophyll hydrolyzing enzymes in plants. Physiol. Mol. Biol. Plants. 22:77–85
Gupta, N., Reddy, K., Bhattacharyya, D., and Chakraborty, S. 2021. Plant responses to Geminivirus infection: guardians of the plant immunity. Virol. J. 18:143
Gutschker, S., Corral, J. M., Schmiedl, A., Ludewig, F., Koch, W., Fiedler-Wiechers, K., Czarnecki, O., Harms, K., Keller, I., Martins Rodrigues, C., Pommerrenig, B., Neuhaus, H. E., Zierer, W., Sonnewald, U., and Müdsam, C. 2022. Multi-omics data integration reveals link between epigenetic modifications and gene expression in sugar beet (Beta vulgaris subsp. vulgaris) in response to cold. BMC Genomics. 23:144
Harrison, B. D. 1985. Advances in Geminivirus research. Annu. Rev. Phytopathol. 23:55–82

Harveson, R. M. 2015. Beet curly top: America's first serious disease of sugar beets. APS Featur. 10

Hoffmann, C. M., Koch, H.-J., and Märländer, B. 2021. Chapter 20 - Sugar beet. Pages 634–672 in: Crop Physiology Case Histories for Major Crops, V.O. Sadras and D.F. Calderini, eds. Academic Press.

Horton, D. R., Cooper, W. R., Grimm, K. S., Crowder, D., Waters, T., Wohleb, C., Frost, K., Jensen, A., and Blua, M. 2018. The beet leafhopper odyssey in North America: a brief overview. Res. Ext. Potato Ind. Ida. Or. Wash. 18

Hu, T., Huang, C., He, Y., Castillo-González, C., Gui, X., Wang, Y., Zhang, X., and Zhou, X. 2019. βC1 protein encoded in geminivirus satellite concertedly targets MKK2 and MPK4 to counter host defense. PLOS Pathog. 15:e1007728

Hudson, A., Richman, D. B., Escobar, I., and Creamer, R. 2010. Comparison of the feeding behavior and genetics of beet leafhopper, circulifer tenellus, populations from California and New Mexico. Southwest. Entomol. 35:241–250

Iriti, M., and Faoro, F. 2008. Abscisic acid is involved in chitosan-induced resistance to tobacco necrosis virus (TNV). Plant Physiol. Biochem. 46:1106–1111

Jongbum, P., Hwang, H., Shim, H., Im, K., Auh, C.-K., Lee, S., and Davis, K. 2004. Altered cell shapes, hyperplasia, and secondary growth in Arabidopsis caused by beet curly top geminivirus infection. Mol. Cells. 17:117–24

Kaffka, S. R., Wintermantel, W. M., and Lewellen, R. T. 2002. Comparisons of soil and seed applied systemic insecticides to control beet curly top virus in the San Joaquin Valley. J. Sugar Beet Res. 39:59–74

Kallenbach, M., Bonaventure, G., Gilardoni, P. A., Wissgott, A., and Baldwin, I. T. 2012. Empoasca leafhoppers attack wild tobacco plants in a jasmonate-dependent manner and identify jasmonate mutants in natural populations. Proc. Natl. Acad. Sci. 109:E1548–E1557

Klessig, D. F., Choi, H. W., and Dempsey, D. A. 2018. Systemic acquired resistance and salicylic acid: past, present, and future. Mol. Plant. Microbe Interact. 31:871–888

Kogan, M., and Ortman, E. F. 1978. Antixenosis-A New Term Proposed to Define Painter's "Nonpreference" Modality of Resistance. Bull. Entomol. Soc. Am. 24:175–176

Lapidot, M., and Friedmann, M. 2002. Breeding for resistance to whitefly-transmitted geminiviruses. Ann. Appl. Biol. 140:109–127

Latham, J. R., Saunders, K., Pinner, M. S., and Stanley, J. 1997. Induction of plant cell division by beet curly top virus gene C4. Plant J. 11:1273–1283

Li, T., Huang, Y., Xu, Z.-S., Wang, F., and Xiong, A.-S. 2019. Salicylic acid-induced differential resistance to the Tomato yellow leaf curl virus among resistant and susceptible tomato cultivars. BMC Plant Biol. 19:173

Liu, S. R., Zhou, J. J., Hu, C. G., Wei, C. L., and Zhang, J. Z. 2017. MicroRNA-mediated gene silencing in plant defense and viral counter-defense. Front. Microbiol. 8:1801

Lozano-Durán, R., Rosas-Díaz, T., Gusmaroli, G., Luna, A. P., Taconnat, L., Deng, X. W., and Bejarano, E. R. 2011. Geminiviruses subvert ubiquitination by altering csn-mediated derubylation of SCF E3 ligase complexes and inhibit jasmonate signaling in Arabidopsis thaliana. Plant Cell. 23:1014–1032

Machado, J. P. B., Calil, I. P., Santos, A. A., and Fontes, E. P. B. 2017. Translational control in plant antiviral immunity. Genet. Mol. Biol. 40:292–304

Macho, A. P., Boutrot, F., Rathjen, J. P., and Zipfel, C. 2012. Aspartate oxidase plays an important role in Arabidopsis stomatal immunity. Plant Physiol. 159:1845–1856
Majumdar, R., Galewski, P. J., Eujayl, I., Minocha, R., Vincill, E., and Strausbaugh, C. A. 2022. Regulatory roles of small non-coding RNAs in sugar beet resistance against beet curly top virus. Front. Plant Sci. 12
Mauck, K. E. 2016. Variation in virus effects on host plant phenotypes and insect vector behavior: what can it teach us about virus evolution? Curr. Opin. Virol. 21:114–123
McGinnis, E. E., Meyer, M. H., and Smith, A. G. 2010. Sweet and sour: A scientific and legal look at herbicide-tolerant sugar beet. Plant Cell. 22:1653–1657
McGrath, J. M., Funk, A., Galewski, P., Ou, S., Townsend, B., Davenport, K., Daligault, H., Johnson, S., Lee, J., Hastie, A., Darracq, A., Willems, G., Barnes, S., Liachko, I., Sullivan, S., Koren, S., Phillippy, A., Wang, J., Liu, T., Pulman, J., Childs, K., Shu, S., Yocum, A., Fermin, D., Mutasa-Göttgens, E., Stevanato, P., Taguchi, K., Naegele, R., and Dorn, K. M. 2023. A contiguous de novo genome assembly of sugar beet EL10 (Beta vulgaris L.). DNA Res. 30:dsac033
Miklas, P. N., Seo, Y.-S., and Gilbertson, R. L. 2009. Quantitative resistance to bean dwarf mosaic virus in common bean is associated with the bct gene for resistance to beet curly top virus. Plant Dis. 93:645–648
Moliterni, V. M. C., Paris, R., Onofri, C., Orrù, L., Cattivelli, L., Pacifico, D., Avanzato, C., Ferrarini, A., Delledonne, M., and Mandolino, G. 2015. Early transcriptional changes in Beta vulgaris in response to low temperature. Planta. 242:187–201
Morel, J. B., and Dangl, J. L. 1997. The hypersensitive response and the induction of cell death in plants. Cell Death Differ. 4:671–683
Mozuraitis, R., Stranden, M., Ramirez, M. I., Borg-Karlson, A.-K., and Mustaparta, H. 2002. (-)-Germacrene D increases attraction and oviposition by the tobacco budworm moth heliothis virescens. Chem. Senses. 27:505–509
Müllender, M., Varrelmann, M., Savenkov, E. I., and Liebe, S. 2021. Manipulation of auxin signaling by plant viruses. Mol. Plant Pathol. 22:1449–1458
Munyaneza, J. E., and Upton, J. E. 2005. Beet leafhopper (hemiptera: cicadellidae) settling behavior, survival, and reproduction on selected host plants. J. Econ. Entomol. 98
Nebapure, S. M., Shankarganesh, K., Rajna, S., Naga, K. C., Pandey, D., Gambhir, S., Praveen, K. V., and Subramanian, S. 2022. Dynamic changes in virus-induced volatiles in cotton modulate the orientation and oviposition behavior of the whitefly Bemisia tabaci. Front. Physiol. 13:1017948
Niu, Y., Han, S., Wu, Z., Pan, C., Wang, M., Tang, Y., Zhang, Q.-H., Tan, G., and Han, B. 2022. A push-pull strategy for controlling the tea green leafhopper (Empoasca flavescens F.) using semiochemicals from Tagetes erecta and Flemingia macrophylla. Pest Manag. Sci. 78:2161–2172
Pagán, I., and García-Arenal, F. 2020. Tolerance of plants to pathogens: a unifying view. Annu. Rev. Phytopathol. 58:77–96
Pagán, I., and García-Arenal, F. 2018. Tolerance to plant pathogens: theory and experimental evidence. Int. J. Mol. Sci. 19:810
Painter, R. H. 1951. Insect resistance in crop plants. Soil Sci. 72:481
Panella, L., Kaffka, S. R., Lewellen, R. T., Mitchell McGrath, J., Metzger, M. S., and Strausbaugh, C. A. 2014. Sugar beet. Pages 357–395 in: Yield Gains in Major U.S. Field Crops, John Wiley & Sons, Ltd.

Pieterse, C. M. J., Van der Does, D., Zamioudis, C., Leon-Reyes, A., and Van Wees, S. C. M. 2012. Hormonal modulation of plant immunity. Annu. Rev. Cell Dev. Biol. 28:489–521

Rojas, C., Senthil-Kumar, M., Tzin, V., and Mysore, K. 2014. Regulation of primary plant metabolism during plant-pathogen interactions and its contribution to plant defense. Front. Plant Sci. 5

Sáez, C., Flores-León, A., Montero-Pau, J., Sifres, A., Dhillon, N. P. S., López, C., and Picó, B. 2022. RNA-Seq transcriptome analysis provides candidate genes for resistance to tomato leaf curl new delhi virus in melon. Front. Plant Sci. 12

Santner, A., and Estelle, M. 2009. Recent advances and emerging trends in plant hormone signaling. Nature. 459:1071–1078

Santos, A., Carvalho, C., Florentino, L., Humberto, J., and Fontes, E. P. B. 2009. Conserved threonine residues within the a-loop of the receptor nik differentially regulate the kinase function required for antiviral signaling. PLOS ONE. 4

Sarwar, M. 2020. Chapter 27 - Insects as transport devices of plant viruses. Pages 381–402 in: Applied Plant Virology, L.P. Awasthi, ed. Academic Press.

Schuh, R. T., and Slater, J. A. 1995. *True Bugs of the World (Hemiptera:Heteroptera): Classification and Natural History*. Cornell University Press.

Sedano, M., Lam, N., Escobar, I., Cross, T., Hanson, S. F., and Creamer, R. 2012. Application of vascular puncture for evaluation of curtovirus resistance in chile pepper and tomato. J. Phytopathol. 160:120–128

Severin, H. H. P. 1946. Longevity, or life histories, of leaf-hopper species on virus-infected and on healthy plants. J. Agric. Sci. Publ. Calif. Agric. Exp. Stn. 17

Sharma, N., Muthamilarasan, M., Dulani, P., and Prasad, M. 2021. Genomic dissection of ROS detoxifying enzyme encoding genes for their role in antioxidative defense mechanism against Tomato leaf curl New Delhi virus infection in tomato. Genomics. 113:889–899

Shen, Q., Hu, T., Bao, M., Cao, L., Zhang, H., Song, F., Xie, Q., and Zhou, X. 2016. Tobacco ring E3 ligase NtRPF1 mediates ubiquitination and proteasomal degradation of a geminivirus-encoded βC1. Mol. Plant. 9:911–925

Shen, Q., Liu, Z., Song, F., Xie, Q., Hanley-Bowdoin, L., and Zhou, X. 2011. Tomato SlSnRK1 protein interacts with and phosphorylates βC1, a pathogenesis protein encoded by a geminivirus β-Satellite. Plant Physiol. 157:1394–1406

Smith, C. M. 2005. *Plant resistance to arthropods molecular and conventional approaches*. Springer.

Soto, M. J., Chen, L. F., Seo, Y. S., and Gilbertson, R. L. 2005. Identification of regions of the beet mild curly top virus (family geminiviridae) capsid protein involved in systemic infection, virion formation and leafhopper transmission. Virology. 341:257–270

Soto, M. J., and Gilbertson, R. L. 2003. Distribution and rate of movement of the curtovirus beet mild curly top virus (family geminiviridae) in the beet leafhopper. Phytopathology. 93:478–484

Stanley, J., Markham, P. G., Callis, R. J., and Pinner, M. S. 1986. The nucleotide sequence of an infectious clone of the geminivirus beet curly top virus. EMBO J. 5:1761–1767

Stenger, D. C., and McMahon, C. L. 1997. Genotypic diversity of beet curly top virus populations in the Western United States. Phytopathology. 87:737–744

Strausbaugh, C. A., Eujayl, I. A., and Wintermantel, W. M. 2017. Beet curly top virus strains associated with sugar beet in Idaho, Oregon, and a Western U.S. collection. Plant Dis. 101:1373–1382

Strausbaugh, C. A., Wenninger, E. J., and Eujayl, I. A. 2014. Control of curly top in sugar beet with seed and foliar insecticides. Plant Dis. 98:1075–1080
Strausbaugh, C. A., Wenninger, E. J., and Eujayl, I. A. 2016. Length of efficacy for control of curly top in sugar beet with seed and foliar insecticides. Plant Dis. 100:1364–1370
Strausbaugh, C. A., Wintermantel, W. M., Gillen, A. M., and Eujayl, I. A. 2008. Curly top survey in the Western United States. Phytopathology. 98:1212–1217
Sugio, A., Kingdom, H. N., MacLean, A. M., Grieve, V. M., and Hogenhout, S. A. 2011. Phytoplasma protein effector SAP11 enhances insect vector reproduction by manipulating plant development and defense hormone biosynthesis. Proc. Natl. Acad. Sci. 108:E1254–E1263
Thomas, P. E. 1972. Mode of expression of host preference by Circulifer tenellus, the vector of curly top virus. J. Econ. Entomol. 65:119–123
Thomas, P. E., and Boll, R. K. 1977. Effect of host preference on transmission of curly top virus to tomato by the beet leafhopper. Am. Phytopathol. Soc. 67:903–905
USDA Crop Values Summary. 2023.
Vinutha, T., Vanchinathan, S., Bansal, N., Kumar, G., Permar, V., Watts, A., Ramesh, S. V., and Praveen, S. 2020. Tomato auxin biosynthesis/signaling is reprogrammed by the geminivirus to enhance its pathogenicity. Planta. 252:51
Wang, Y., Wu, Y., Gong, Q., Ismayil, A., Yuan, Y., Lian, B., Jia, Q., Han, M., Deng, H., Hong, Y., Hanley-Bowdoin, L., Qi, Y., and Liu, Y. 2019. Geminiviral V2 protein suppresses transcriptional gene silencing through interaction with AGO4. J. Virol. 93:e01675-18
Weeks, M. 2017. Sugar state: industry, science, and the nation in Colorado's sugar beet fields. West. Hist. Q. 48:367–391
Wintermantel, W. M. 2005. Co-infection of beet mosaic virus with beet yellowing viruses leads to increased symptom expression on sugar beet. Plant Dis. 89:325–331
Wintermantel, W. M., and Kaffka, S. R. 2006. Sugar beet performance with curly top is related to virus accumulation and age at infection. Plant Dis. 90:657–662
Wood, T. J., and Goulson, D. 2017. The environmental risks of neonicotinoid pesticides: a review of the evidence post 2013. Environ. Sci. Pollut. Res. Int. 24:17285–17325
Wu, X., Valli, A., García, J. A., Zhou, X., and Cheng, X. 2019. The tug-of-war between plants and viruses: great progress and many remaining questions. Viruses. 11:203
Yu, C. Y., and Kanehara, K. 2020. The unfolded protein response modulates a phosphoinositide-binding protein through the IRE1-bZIP60 Pathway. Plant Physiol. 183:221–235
Zaidi, S. S.-A., Naqvi, R. Z., Asif, M., Strickler, S., Shakir, S., Shafiq, M., Khan, A. M., Amin, I., Mishra, B., Mukhtar, M. S., Scheffler, B. E., Scheffler, J. A., Mueller, L. A., and Mansoor, S. 2020. Molecular insight into cotton leaf curl geminivirus disease resistance in cultivated cotton (Gossypium hirsutum). Plant Biotechnol. J. 18:691–706
Zhang, J., Ma, M., Liu, Y., and Ismayil, A. 2023. Plant defense and viral counter-defense during plant–geminivirus interactions. Viruses. 15:510
Zhang, L., Zhang, F., Melotto, M., Yao, J., and He, S. Y. 2017. Jasmonate signaling and manipulation by pathogens and insects. J. Exp. Bot. 68:1371–1385
Zou, C., Guo, Z., Zhao, S., Chen, J., and Zhang, C. 2023. Identification and functional prediction of CircRNAs involved in drought responses in sugar beet (Beta vulgaris L.). Sugar Tech. 25:1152–1166

Zou, C., Liu, D., Wu, P., Wang, Y., Gai, Z., Liu, L., Yang, F., Li, C., and Guo, G. 2020. Transcriptome analysis of sugar beet (Beta vulgaris L.) in response to alkaline stress. Plant Mol. Biol. 102:645–657

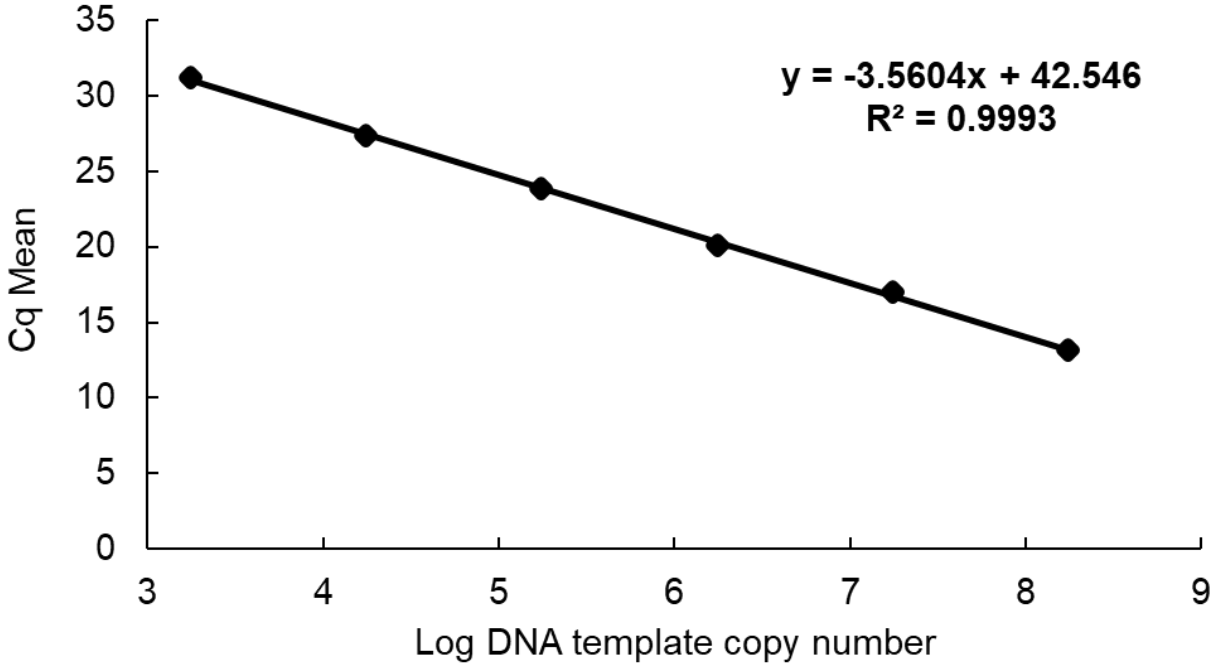

Supplementary Figure 1: Standard curve of BCTV plasmid construct based on mean Cq values obtained from a ten-fold dilution series with DNA copy numbers ranging from 1.7 x 10^8 to 1.7 x 10^3. The primer efficiency was determined to be 91%. This standard curve was used to calculate the average number BCTV coat protein copies in each plant genotype over time.

Supplemental Table 1: Statistical test used and *p*-values for feeding choice preference assays. Bold values indicate significant *p*-value < 0.05.

Timepoint	Statistical Test	Uninfected Leafhoppers *p* -value	Virus-Infected Leafhoppers *p* -value
Whole data set	Friedman-Kruskal (Kruskal.test)	**1.97E-11**	**0.0068**
1 hour	Wilcoxon rank sum test (wilcox.test)	0.7977	0.5239
2 hour	Wilcoxon rank sum test (wilcox.test)	0.114	0.6666
4 hour	Wilcoxon rank sum test (wilcox.test)	**0.0052**	0.7393
6 hour	Wilcoxon rank sum test (wilcox.test)	**0.0039**	0.8238
12 hour	Wilcoxon rank sum test (wilcox.test)	**0.0015**	0.1829
24 hour	Wilcoxon rank sum test (wilcox.test)	**0.0118**	**0.0036**
36 hour	Wilcoxon rank sum test (wilcox.test)	**0.0028**	0.9888
48 hour	Wilcoxon rank sum test (wilcox.test)	**0.0021**	**0.0236**

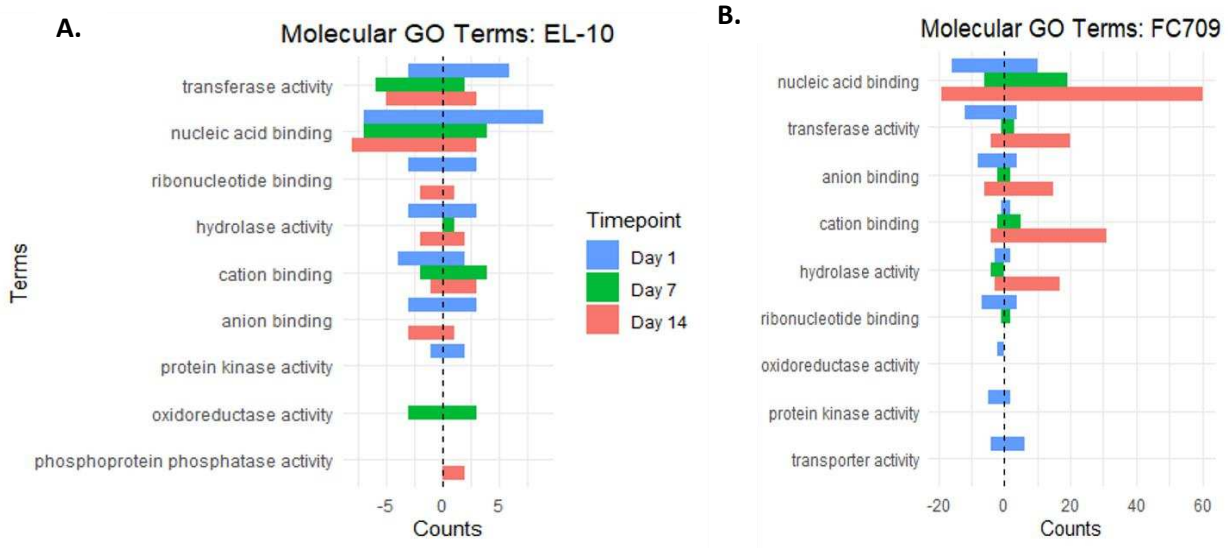

Supplemental Figure 2: Molecular gene ontology (GO) terms for mock-inoculated vs BCTV-inoculated comparisons for **(A)** EL10 and **(B)** FC709-2 at each timepoint. Each bar shows the number of up and down regulated transcript counts under each parent term.

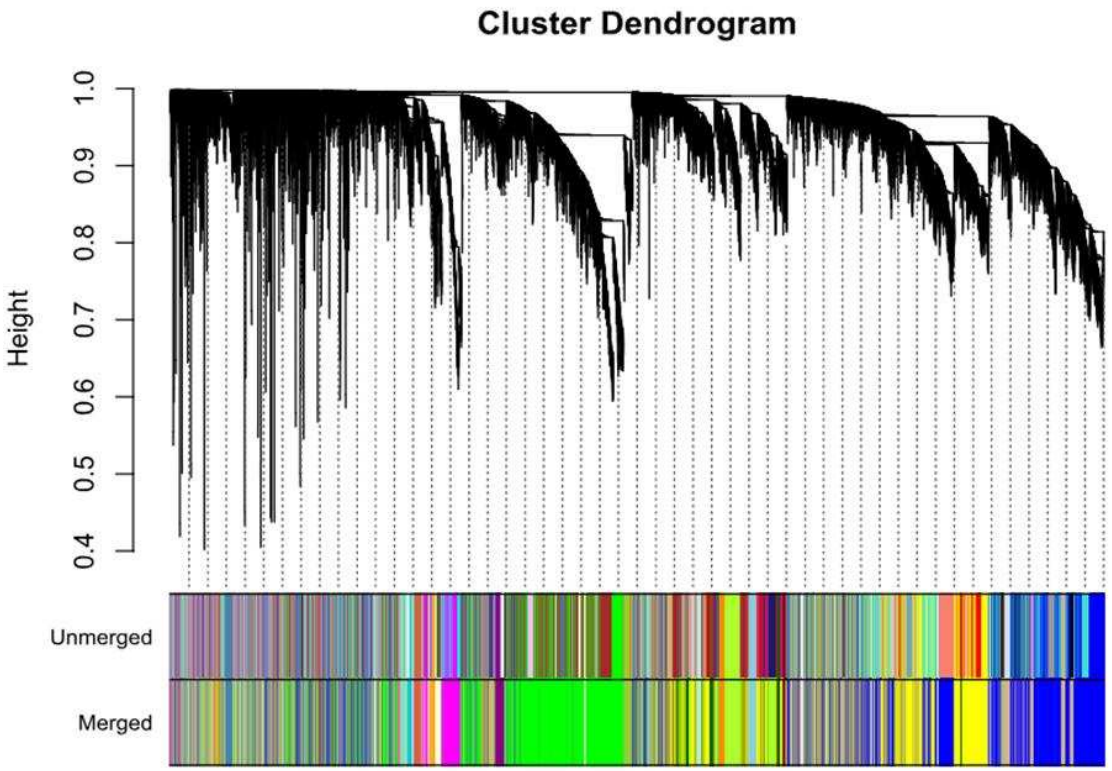

Supplemental Figure 3: Weighted gene co-expression network analysis (WGCNA) of sugar beet transcripts identified in BCTV infected and uninfected leaf samples at different timepoints. The cluster dendrogram shows each module, represented by the different colors, before (unmerged) and after (merged) combining the modules of 75% shared identity.